Ketamine's pharmacogenomic network in human brain contains sub-networks associated with glutamate neurotransmission and with neuroplasticity

One Sentence Summary: The ketamine network in the human brain consists of sub-networks associated with glutamate neurotransmission, neuroplasticity, and pharmacokinetics.

Authors: Gerald A. Higgins[1, 2], Samuel A. Handelman[3], Ari Allyn-Feuer[1]†, Alex S. Ade[1, 2], James S. Burns[2], Gilbert S. Omenn[1, 3, 4, 5], Brian D. Athey[1, 2, 6]*

Affiliations:

[1]Department of Computational Medicine and Bioinformatics, University of Michigan Medical School, Ann Arbor, MI 48109, USA.

[2]Phenomics Health Inc., Ann Arbor, MI 48109, USA.

[3]Department of Internal Medicine, University of Michigan Medical School, Ann Arbor, MI 48109, USA.

[4]School of Public Health, University of Michigan, Ann Arbor, MI 48109, USA.

[5]Department of Human Genetics, University of Michigan Medical School, Ann Arbor, MI 48109, USA.

[6]Department of Psychiatry, University of Michigan Medical School, Ann Arbor, MI 48109, USA.

*Corresponding author: Email: bleu@med.umich.edu (B.D.A.)

†Current address: GlaxoSmithKline, King of Prussia, PA 19406, USA.

Abstract: The pharmacogenomic network responsible for the rapid antidepressant action of ketamine and concomitant adverse events in patients has been poorly defined. Integrative, multi-scale biological data analytics helps explain ketamine's action. Using a validated computational pipeline, candidate ketamine-response genes and regulatory RNAs from published literature, binding affinity studies, and single nucleotide polymorphisms (SNPs) from genomewide association studies (GWAS), we identified 108 SNPs associated with 110 genes and regulatory RNAs. All of these SNPs are classified as enhancers, and additional chromatin interaction mapping in human neural cell lines and tissue shows enhancer-promoter interactions involving other network members. Pathway analysis and gene set optimization identified three composite sub-networks within the broader ketamine pharmacogenomic network. Expression patterns of ketamine network genes within the postmortem human brain are concordant with ketamine neurocircuitry based on the results of 24 published functional neuroimaging studies. The ketamine pharmacogenomic network is enriched in forebrain regions known to be rapidly activated by ketamine, including cingulate cortex and frontal cortex, and is significantly regulated by ketamine (p=6.26E-33; Fisher's exact test). The ketamine pharmacogenomic network can be partitioned into distinct enhancer sub-networks associated with: (1) glutamate neurotransmission, chromatin remodeling, smoking behavior, schizophrenia, pain, nausea, vomiting, and post-operative delirium; (2) neuroplasticity, depression, and alcohol consumption; and (3) pharmacokinetics. The component sub-networks explain the diverse action mechanisms of ketamine and its analogs. These results may be useful for optimizing pharmacotherapy in patients diagnosed with depression, pain or related stress disorders.

Introduction

Existing antidepressant medications are not effective for many patients (*1*). Novel antidepressant drugs include compounds that target the N-methyl-d-aspartate receptor (NMDAR), glycine receptor, or the α-amino-3-hydroxy-5-methyl-4-isoxazolepropionic acid receptor (AMPAR) in the human brain. For example, ketamine (*RS*-2-chlorophenyl-2-methylamino-cyclohexanone), a noncompetitive NMDAR antagonist first approved by the U.S. Food & Drug Administration (FDA) as a surgical anesthetic in 1970 (*2*), is being increasingly used to treat refractory depression (*3, 4*). There is evidence that the widespread action of ketamine in the human brain impacts a number of pharmacodynamic targets including AMPARs, cholinergic receptors, calcium channels and other neurotransmitter molecules, although most evidence suggests that ketamine and its analogs exert their actions through partial antagonism of the NMDAR in the human brain (*5*-*8*). One presumptive target for ketamine-like drugs is the NMDAR, which also contains binding sites for glycine and D-serine encoded by *GLRB*, and sites that bind polyamines, histamine, and cations. Neuroimaging studies have demonstrated that intravenous infusion of ketamine causes a transient surge in glutamate levels detected in prefrontal cortex and cingulate cortex in parallel with its rapid antidepressant action (*5, 7*).

A 2018 review provided detailed evidence of the therapeutic mechanisms of ketamine, its enantiomers, and active metabolites (*8*). Research suggests that ketamine's antidepressant action might result from stimulation of dendritic spine plasticity in the prefrontal cortex (*9*) or through activation of the inflammasome (*10*). Ketamine and its metabolites also act as modulators of the opiate, cannabinoid, and related receptors (*8*), the hyperpolarization activated cyclic nucleotide gated potassium channel (*11*), the estrogen receptor, and the AMPA receptor subunits GRIA1 and

GRIA4 (*12*), and many other known (*8, 13*) and unknown pharmacodynamic targets within human brain. Ketamine and its metabolites strongly induce the expression of the *CYP2B6* gene in human brain, which encodes a drug metabolizing enzyme that contributes to first- and second-pass metabolism of the drug and its metabolites (*14*). Recent genomewide association studies (GWAS) in humans demonstrate association of ketamine response and adverse events with enhancers of genes and long non-coding RNAs (lncRNAs) related to the roundabout guidance receptor 2 (*ROBO2*) gene, whose product binds members of the slit guidance ligand family (*SLIT1, SLIT2*) that are involved in dendrite guidance and synaptic plasticity (*15, 16*). Like phencyclidine, a structurally related compound, ketamine induces acute dissociation, with both drugs exhibiting species-specific differences in response. In sum, the central nervous system (CNS) pathway(s) responsible for the rapid antidepressant effects of ketamine and its enantiomers in patients diagnosed with treatment-resistant depression (TRD) remain poorly defined, including emergence of on- and off-target effects and individual differences in response and adverse events.

Problematic adverse events that characterize response to ketamine in humans include acute psychological effects such as dissociation, delirium, and cognitive impairment. The drug's dissociative psychotropic effects have emerged as a mechanism to explain the analgesic, anesthetic and sedative effects of ketamine (*1*). Both the racemic and enantiomeric formulations of ketamine produce potent and undesirable psychotomimetic adverse events, including acute sensory distortions, derealization, depersonalization, identity confusion, identity alteration, amnesia, hallucinations, anxiety, and fear (*2, 5, 7, 8*). Dysphoric emergence phenomena occur in a dose-dependent manner, while transient phenomena include elevated blood pressure and heart rate, nausea, and vomiting (*6, 8*).

Intravenous and oral formulations of ketamine have demonstrated efficacy and tolerability in controlled trials and in open-label studies across patient populations known to have little to no response from traditional antidepressants (*6-8*). The *S*-enantiomer of ketamine (Esketamine; Spravato™) has been approved by the U.S. FDA as a nasal spray to be used in combination with a serotonin reuptake inhibitor-based antidepressant for patients who have been diagnosed with TRD (*4*). Esketamine has been approved only for administration by a healthcare professional in a clinical setting because it may produce acute adverse events. In sum, ketamine and its analogs are promising therapeutics for patients diagnosed with depression, but it is uncertain how this powerful psychotropic exerts its widespread response and adverse effects in the human brain (*9, 10, 17-21*).

Our strategy analyzed disparate data from multiple scales of biological function combining bioinformatics, computational medicine and machine learning (*22-25*). GWAS SNPs provided insight into the phenotypic consequences of the mutational alterations and variation within disease sub-networks impacted by ketamine, spatial interactions within chromatin that control expression of ketamine-response genes, and mesoscale functional neurocircuits within human brain regions that are rapidly activated following ketamine administration **(Figure 1)**. We hypothesized that the mechanisms of the different on- and off-target effects of ketamine enantiomers could be determined from studies of disease risk and pharmacogenomic variation in the regulatory, non-coding genome or "regulome" (*23*, *26*). Most GWAS SNPs are located within enhancers in the three-dimensional (3D) spatial genome and allele-specific open chromatin provides the foundation on which a SNP may impact gene expression and pharmacogenomic variation among humans (*27-29*). This general feature provides a basis for the machine learning algorithms used in this study to determine the putative causal nature of SNPs. If a variant SNP is silenced by heterochromatin

or is located within euchromatin on an allele shrouded by chromatin, it cannot permit the activation of gene expression by transcription factors. Recent studies demonstrate that the topology of the human genome determines regions of activation and repression of gene transcription and translation, organized into enhancer-promoter and promoter-promoter loops in chromatin and long range interactions mediated by superenhancers, topologically associating domains (TADs), and A and B compartments in chromatin (*30, 31*).

To understand if enhancer networks are active in the same human brain regions where ketamine first exerts a rapid antidepressant response, we determined whether the expressed target genes and their enhancer networks are concentrated within these regions of the CNS. This was accomplished by matching ketamine pharmacogenomic gene expression with higher-order structures where the drug first acts in the human brain, determining whether the GWAS SNPs associated with ketamine's sub-networks act in these CNS regions, and assessing whether enhancer and superenhancer regulatory elements are localized to this circumscribed neuroanatomical substrate **(Figure 1)**.

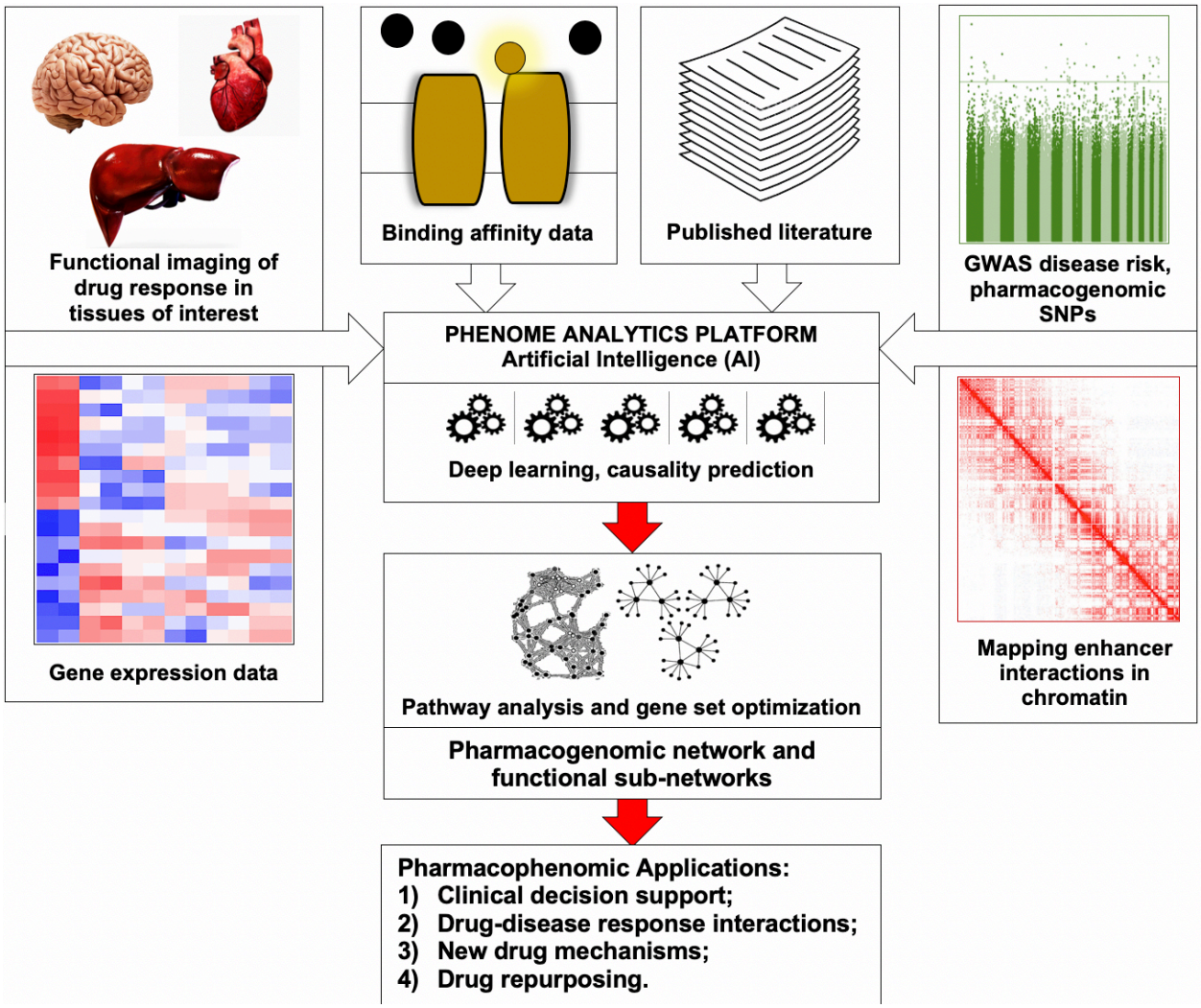

Figure 1. Multi-scale biological data analysis. This strategy for mapping drug networks provides insight into the *mechanistic* on- and off-target effects, laying a foundation for subsequent preclinical studies.

Results

The ketamine pharmacogenomic network in the human brain

The ketamine pharmacogenomic network we identified consists of 110 genes and regulatory RNAs and exhibits significant overlap with the "cardiovascular disease, neurological disease and organismal injury abnormalities" disease network category as determined using IPA™ (*32*) (p=1E-54; Fisher's exact test). The proteins encoded by the genes in the network exhibit statistically significant STRING sub-network associations (*data not shown*) (*33*). The top 10 most significant biological processes determined by the Panther/Gene Ontology database (*34*) include trans-synaptic signaling, regulation of membrane potential, behavior, response to drug, and nervous system development. The most significant upstream xenobiotic regulator of the network is ketamine at p=6.26E-33 (*32, 35*). The top 10 disease gene risk variant categories enriched in the ketamine pharmacogenomic network include cognitive impairment, dissociative disorder, and mood disorders. These results point to a ketamine pharmacogenomic network in the human CNS, because the most significant biological functions of the network are consistent with what is known about ketamine's mechanisms, including NMDAR and glutamate neurotransmission (*5-9*). The ketamine pharmacogenomic network genes and regulatory RNAs exhibit circumscribed localization within 41 TADs, or less than 2% of human TADs (*36*).

Component sub-networks of the ketamine pharmacogenomic network

Gene set optimization resulted in 2 distinctly different sub-networks. The glutamate receptor sub-network is enriched for synaptic signaling, glutamate receptor signaling, glutamate pathway regulation and chromatin organization. The top xenobiotic (chemical-drug) up-regulator of the

glutamate receptor sub-network is ketamine at p=2.1E-09 **(Figure 2A)** (*32, 35*). In contrast, the neuroplasticity sub-network is enriched for regulation of nervous system development, regulation of neurogenesis, regulation of neuronal differentiation, neurogenesis and nervous system development **(Figure 2B)** (*34*). The neuroplasticity sub-network exhibits significant overlap with the "cardiovascular disease, neurological disease and organismal injury abnormalities" network category as determined by IPA™ (*32*) at *p*=1E-59 and its top xenobiotic up-regulator is also ketamine at *p*=6E-12 **(Figure 4)** (*32, 35*).

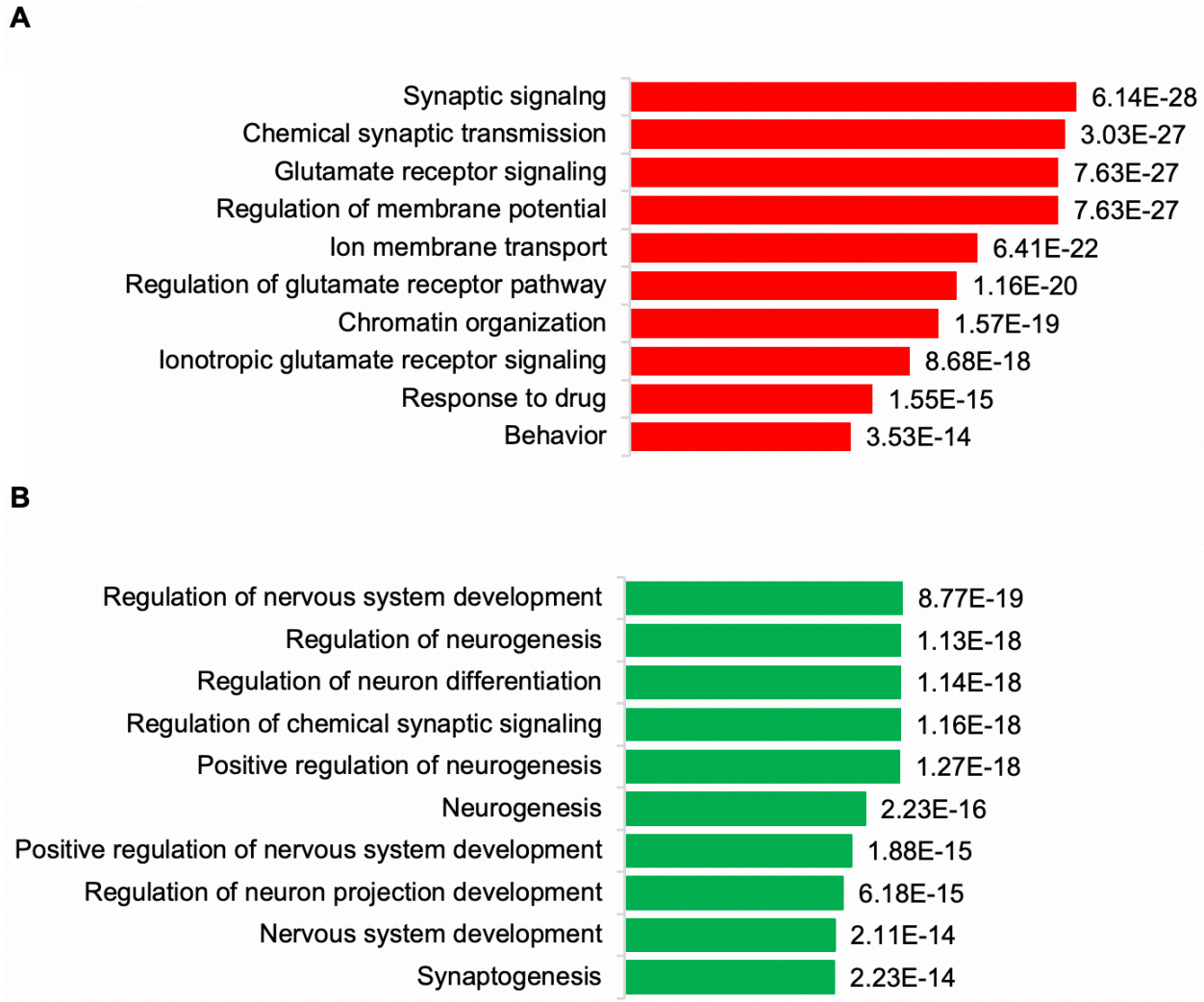

Figure 2. The 10 most significant biological processes from Gene Ontology for the two out of three ketamine pharmacogenomic sub-networks in human brain. (A) The ketamine glutamate receptor sub-network; (B) The ketamine neuroplasticity receptor sub-network. Statistical enrichment using GO (*34*) for "*Homo sapiens*" and "nervous system."

The ketamine glutamate receptor sub-network

Our computational pipeline, based on ketamine-response genes selected from published results, showed differences in disease risk annotation between the glutamate receptor sub-network and the neuroplasticity sub-network, even though the products of both sub-networks are regulated by ketamine. Pathway analysis shows that the glutamate receptor sub-network is significantly associated with cognitive impairment, bipolar disorder, postoperative delirium, schizophrenia affective disorder, schizophrenia, non-cancer pain, postoperative pain, vomiting, nausea, and unconsciousness **(Figure 3)**.

Analysis of glutamate receptor sub-network genes using Gene Ontology (*31*) for human CNS biological processes shows the genes *CACNA1C, CACNB2, DLG4*, *GRIN1, GRIN2A, GRIN2B, GRIN2C, GRIN2D, GRIN3A* are significantly enriched for NMDA glutamate neurotransmission. The genes *SETDB1, TRIM28* and *ZNF274* are enriched for chromatin remodeling in neuronal differentiation, and *BRD1, EHMT1* and *MBD1* are enriched for histone 3 lysine 9 (H3K9) methylation. Different bioinformatic applications (*32-35*) and GWAS disease risk and pharmacogenomic SNP annotations (*37*) showed that essential genes associated with cognitive impairment include *ATFIP*, *BORCST*, *GRIA4* and *GAD1*. Mutations in the calcium channel gene *CACNA1C* has been significantly associated with schizophrenia spectrum disorders, including bipolar I disorder, as have *CACNB2*, *GRIN2A* and *HCN1* **(Supplementary Table 4)**. Post-operative delirium has been associated with the expression of *ACHE, CHRM2, GABRA2, GABRA5, GLRA1, GLRB, GRIA1*, including genes that encode the protein constituents of the NMDA receptor. Nausea and vomiting, common side effects of ketamine therapy, have been associated with cholinergic and opiate gene expression.

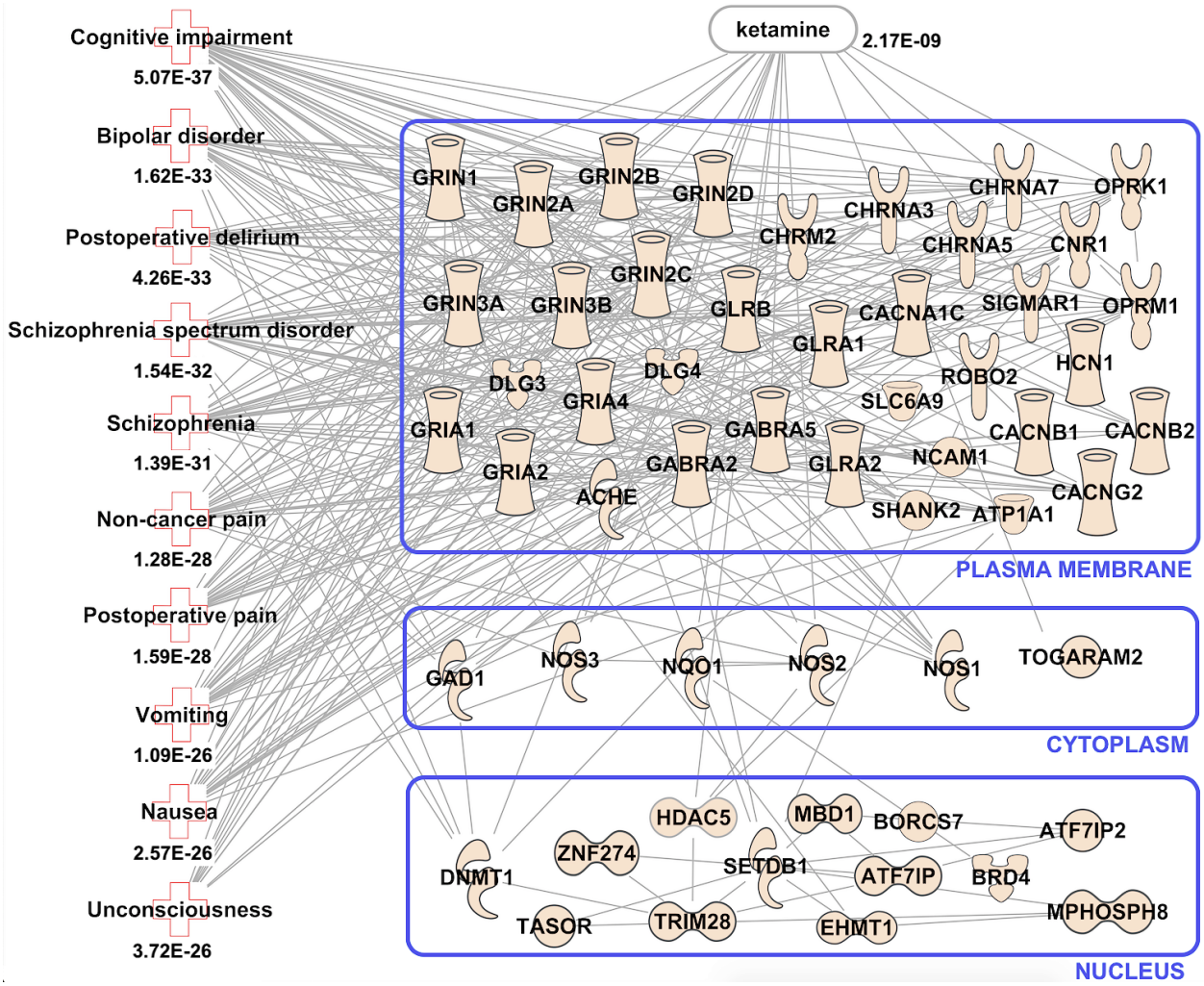

Figure 3. Diseases and conditions associated with the ketamine pharmacogenomic glutamate receptor sub-network, based on the published literature, and visualized using IPA™ (*32*). Lines between the symbols indicate significant interconnectivity as defined by IPA™ (*32*), STRING (*33*) and KEGG (*35*), but do not provide information about the nature of the relationships between genes, their protein products, or regulatory RNAs. **Supplementary Table 2A** lists the gene definitions for the members of the ketamine glutamate receptor sub-network. **Key to gene symbols:**

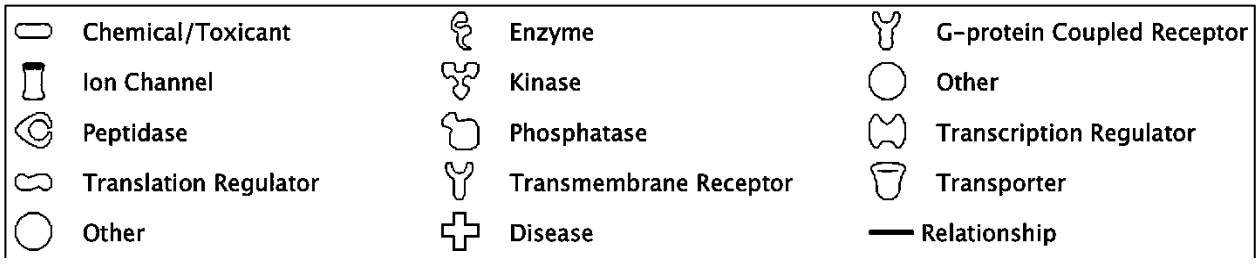

The ketamine neuroplasticity sub-network

The neuroplasticity sub-network is significantly associated with emotional behavior, abnormal morphology of the nervous system, abnormal morphology of brain, depression, anxiety, and abnormal morphology of neurons **(Figure 4)**. Enrichment of sub-network members using Gene Ontology (*31*) for human CNS biological processes associates the genes *ARC, CAMK2A, CNR1, ROBO2, SEMA3A, SLT1* and *SLIT* with synaptic and dendritic plasticity, and *ASCL1, CUX2, BDNF, DCC, KLF6, NEUROD1, NEUROD2, NHLH2, SYN1, SYN2, TBR1* and *TCF4* with neurogenesis.

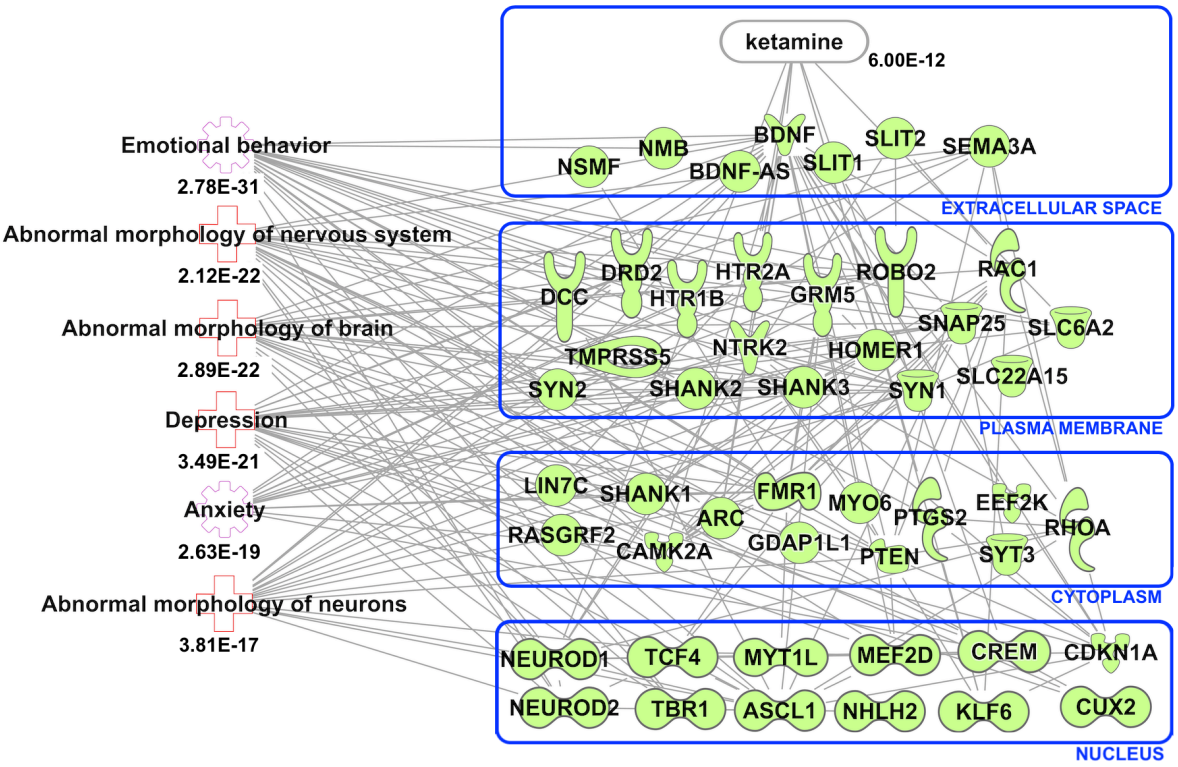

Figure 4. Diseases and conditions associated with the ketamine neuroplasticity sub-network, based on the published literature, and visualized using IPA™ (*32*). Lines between the symbols indicate significant interconnectivity as defined by IPA™ (*32*), STRING (*33*) and KEGG (*35*), but do not provide information about the nature of the relationships between genes, their protein products, or regulatory RNAs. **Supplementary Table 2B** lists the gene definitions for the members of the ketamine glutamate receptor sub-network. The Key for the symbols in this figure is shown in the caption of **Figure 3**.

The ketamine pharmacokinetic sub-network

A third pharmacokinetic sub-network contains genes that encode cytochrome P450 enzymes, *CYP2B6, CYP2A6* and *CYP3A4*, whose products are responsible for the metabolism of ketamine enantiomers (*8, 12*). This sub-network also contains the *ESR1* gene, which encodes the estrogen receptor alpha subunit (*37*), and *TCERG1*, which encodes a nuclear protein that regulates transcriptional elongation and pre-mRNA splicing (*38*) **(Figure 5)**. The ketamine pharmacokinetic sub-network also contains genes from the other sub-networks, including *ANAPC2, DLG4, EFF2K, GRIA1, GRIA4, GRIN1, GRIN2B, MYO6* and *ROBO2*, so is not significantly different from the other two ketamine sub-networks.

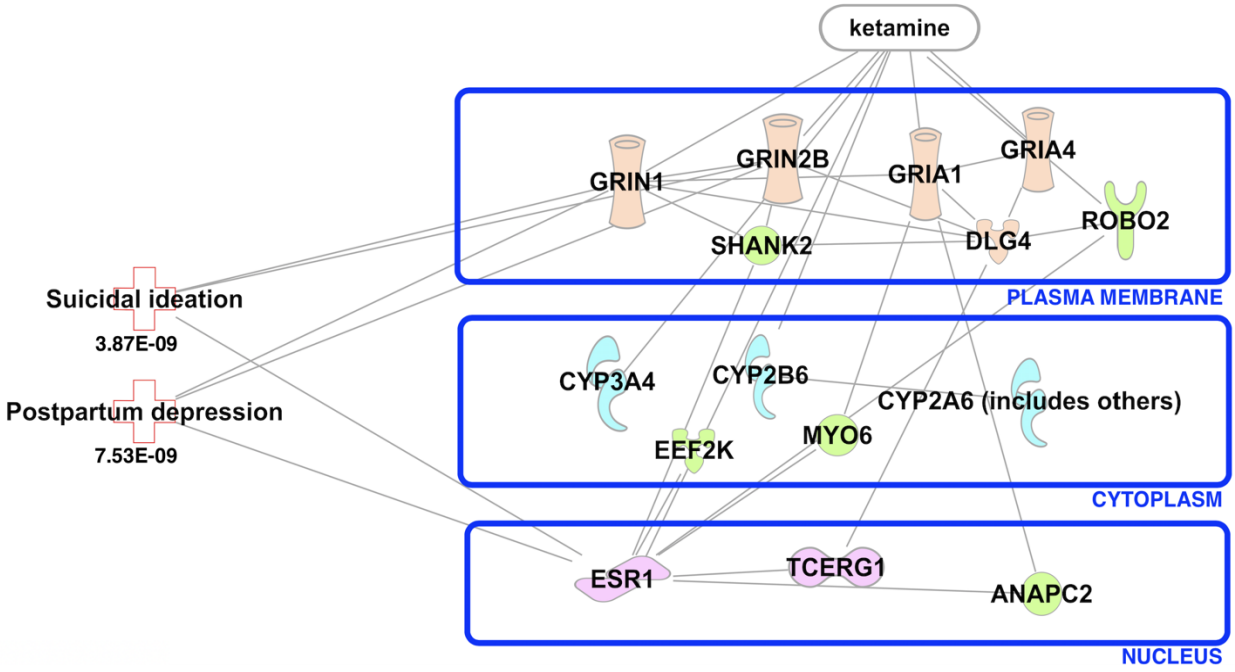

Figure 5. Diseases and conditions associated with the ketamine neuroplasticity sub-network, based on the published literature, and visualized using IPA™ (*32*). Lines between the symbols indicate significant interconnectivity as defined by IPA™ (*32*), STRING (*33*) and KEGG (*35*), but do not provide information about the nature of the relationships between genes, their protein products, or regulatory RNAs. **Supplementary Table 2C** lists the gene definitions for the members of the ketamine glutamate receptor sub-network. The Key for the symbols in this figure is shown in the caption of **Figure 3**. **Supplementary Table 2C** lists the gene definitions for the members of the ketamine glutamate receptor sub-network. The Key for the symbols is shown in the caption of **Figure 3**.

GWAS disease risk SNPs and Hi-C loops discriminate 2 ketamine sub-networks

We hypothesized that psychiatric and social genotype-phenotype associations from GWAS may be useful in the functional characterization of the effects of ketamine in humans, in addition to published GWAS SNPs associated with dissociation and antidepressant measures in response to ketamine (*15, 37*). Because the majority of GWAS SNPs are located within intergenic and intragenic enhancers (*28, 30, 38*) we tested whether GWAS disease risk located within the ketamine glutamate receptor and ketamine neuroplasticity sub-networks were likely to be located within chromatin loops in neural cells (SK-N-SH, H1, A735 cell lines and postmortem brain). If the GWAS SNPs contained in the sub-networks were predicted to be causal in the appropriate human surrogate tissue types, either neural (SK-N-SH, H1) or astrocyte (A735) cells but not in a liver cell line (HepG2) or in a white blood cell using multiple machine learning algorithms (*39-45*), they were used to probe public Hi-C datasets using a bioanalytic method developed in our laboratory (*46*) **(Materials and Methods)**.

We found a total of 186 disease and pharmacogenomic association signals for SNPs predicted to be causal within the ketamine glutamate receptor sub-network and within the ketamine neuroplasticity sub-network. These 186 signals correspond to 108 non-overlapping SNPs and 78 SNPs were significantly associated with at least two traits. The 78 multi-trait SNPs were located either in the ketamine glutamate receptor sub-network or the ketamine neuroplasticity sub-network, but not in both sub-networks. Machine learning predicted that all of the sub-network SNPs were causal. The threshold for predicted causality required consensus of the numerical scores output from five different machine learning algorithms (*39-44*) and a deep learning software application (*45*) **(Materials and Methods)**. When compared to the scores generated from a

random selection of ten GWAS SNPs for all human traits with *p*-values at 5E-08 or lower, every score for each of the GWAS SNPs contained within these two sub-networks was designated as casual **(Supplementary Table 4, Supplementary Table 5)**. Phenotype associations were carefully evaluated from source publications to eliminate those that were entirely self-reported or were ambiguous in terms of assignment to a coded psychiatric disorder (*37, 47*). The 186 GWAS signals associated with genes and regulatory RNAs that were members of the ketamine pharmacogenomic sub-networks identified in this study were annotated by disease risk, psychiatric subtype, enhancer, eQTL, Hi-C score (from both public data and our own adjustable bin mapping method) and co-localization with enhancer RNA. These 186 signals comprised 108 unique GWAS disease risk and pharmacogenomic SNPs predicted to be casual, including 78 SNPs with signals for multiple traits, exhibited clear genotype-phenotype association differences that discriminated the ketamine glutamate receptor sub-network from the ketamine neuroplasticity sub-network **(Table 1)**, although there was overlap for certain genetic associations including schizophrenia and smoking and recurrent depression **(Supplementary Table 4, Supplementary 5).**

Table 1A shows that multiple GWAS disease risk SNPs located within the glutamate receptor sub-network can be annotated as enhancers associated with tobacco smoking status, chronic schizophrenia (ICD diagnostic code F20), and bipolar 1 disorder (ICD diagnostic codes F31.0 – F31.64). **Table 1B** shows that the ketamine neuroplasticity sub-network contains multiple GWAS disease risk SNPs that can be annotated as enhancers associated with recurrent depression (ICD code F33), alcoholism and response to ketamine. The results shown in **Table 1**, **Supplementary Table 4**, and **Supplementary Table 5** demonstrate that enhancer SNPs co-localize with a limited number of genes within each sub-network.

A. The ketamine glutamate receptor sub-network							
GWAS SNP	**Populations**	**Gene(s)**	**Reported trait**	**Reported P-value**	**Enhancer, cell type**	**Hi-C score: Human brain**	**PMID**
rs1051730	ASN, EUR	*CHRNA5, CHRNA3*	Smoking status	6E-121	Neuron	1E-27: Nucleus accumbens	30617275
rs28681284	ASN	*CHRNA5, CHRNA3*	Schizophrenia, chronic (F20)	6E-13	Neuron	1E-27: Nucleus accumbens	30285260
rs2007044	ASN	*CACNA1C*	Schizophrenia, chronic (F20)	6E-20	Bipolar neuron	1E-10: Cingulate cortex	29483656
rs7192140	EUR	*GRIN2A*	Smoking status	2E-15	Bipolar neuron	1E-19: Frontal cortex	30643251
rs11647445	EUR	*GRIN2A*	Bipolar I disorder (F31.0 - F31.64)	1E-10	Bipolar neuron	1E-19: Frontal cortex	31043756
rs7893279	ASN, EUR	*CACNB2*	Schizophrenia, chronic (F20)	9E-14	Neuron	1E-10: Frontal cortex	30285260
rs111294930	EUR	*LINC01470, GRIA1*	Schizophrenia, chronic (F20)	9E-12	Bipolar neuron	1E-12: Cingulate cortex	29483656
rs9292918	ASN	*HCN1*	Schizophrenia, chronic (F20)	4E-11	Bipolar neuron	1E-10: Frontal cortex	28991256
rs62367520	EUR	*HCN1*	Smoking status	1E-10	Bipolar neuron	1E-10: Frontal cortex	29283656
B. The ketamine neuroplasticity sub-network							
GWAS SNP	**Populations**	**Gene(s)**	**Reported trait**	**Reported P-value**	**Enhancer, cell type**	**Hi-C score: Human brain**	**PMID**
rs61902811	EUR	*TMPRSS5, DRD2*	Recurrent depression (F33)	4E-39	Neuron	1E-04: Hippocampus	30718901
rs4936277	EUR	*TMPRSS5, DRD2*	Alcohol use disorder, alcohol dependence	1E-13	Bipolar neuron	1.00E-06: Nucleus Accumbens	29942085
rs7227069	EUR	*DCC*	Recurrent depression (F33)	2E-28	Neuron	1E-10: Cingulate cortex	30718901
rs12967143	EUR	*TCF4*	Recurrent depression (F33)	2E-27	Neuron	1E-10: Frontal cortex	30718901
rs7932640	EUR	*GRM5*	Recurrent depression (F33)	3E-25	Neuron	1E-04: Cingulate cortex	30718901
rs139438618	AFR	*SEMA3A*	Major depression and alcoholism	2E-11	Bipolar neuron	1E-10: Nucleus Accumbens	29071344
rs775766	EUR	*ROBO2*	Recurrent depression (F33)	2E-08	Neuron	1E-14: Cingulate cortex	29942085
rs1400237	EUR	*ROBO2*	Response to ketamine in depression	8E-06*	Neuron	1E-14: Cingulate cortex	30552316

Table 1. Selected GWAS SNPs determined to be causal and annotated as enhancers located within (A) the ketamine glutamate receptor sub-network, and (B) the ketamine neuroplasticity sub-network. Data sources used for GWAS and SNP annotation: columns 1-5, the NHGRI-EBI GWAS catalogue (*37*), column 6, enhancer status determined using annotation from (*38, 48-60*), and column 7 using Hi-C data from (*46, 61, 62*). eQTL data support the results shown in column 7 *(63, 64)*. PMID in column 8 indicates PubMed identification number (*65*). All the GWAS SNPs analyzed can be found in **Supplementary Table 4** and **Supplementary Table 5**. *Significance increased by network boosting *(66)*.

The ketamine glutamate receptor sub-network contains SNPs that occur with greatest frequency in association with *CHRNA3, CHRNA5, NCAM1, NOS3, CACN1AC, CACNB2, HCN1,* an intergenic region between *GRIA1 and LINC01470* and *GRIN2A*. The ketamine neuroplasticity sub-network contains SNPs that occur with greatest frequency in association with *TCF4, DCC,* an intergenic region between *DRD2* and *TRMPSS5*, and *GRM5*. These results demonstrate that mutational alteration of enhancer interactomes discriminate between the ketamine glutamate receptor sub-network (chronic schizophrenia, smoking status) and the ketamine neuroplasticity sub-network (recurrent unipolar depression, alcohol consumption).

Ketamine enhancers are preferentially located in the cingulate cortex and the frontal cortex

The distribution of GWAS SNPs, enhancer, super-enhancer, and chromatin spatial contacts are concentrated within the cingulate cortex and the frontal cortex for both the glutamate receptor sub-network and the neuroplasticity sub-network. **Figure 6** shows the neuroanatomical distribution of the 108 GWAS SNPs located within Hi-C loops in either the ketamine glutamate receptor or ketamine neuroplasticity sub-networks based on the published literature (*46, 61, 62)*. These results, combined with correlative mapping of gene expression within these sub-networks based on data from the human brain atlas of the Allen Brain Science Institute (*67*) and functional neuroimaging results from 24 studies of ketamine's rapid antidepressant response **(Supplementary Table 1)**, support research demonstrating that cingulate cortex and frontal cortex are primary sites where the drug exerts its pharmacodynamic effects (*68, 69*).

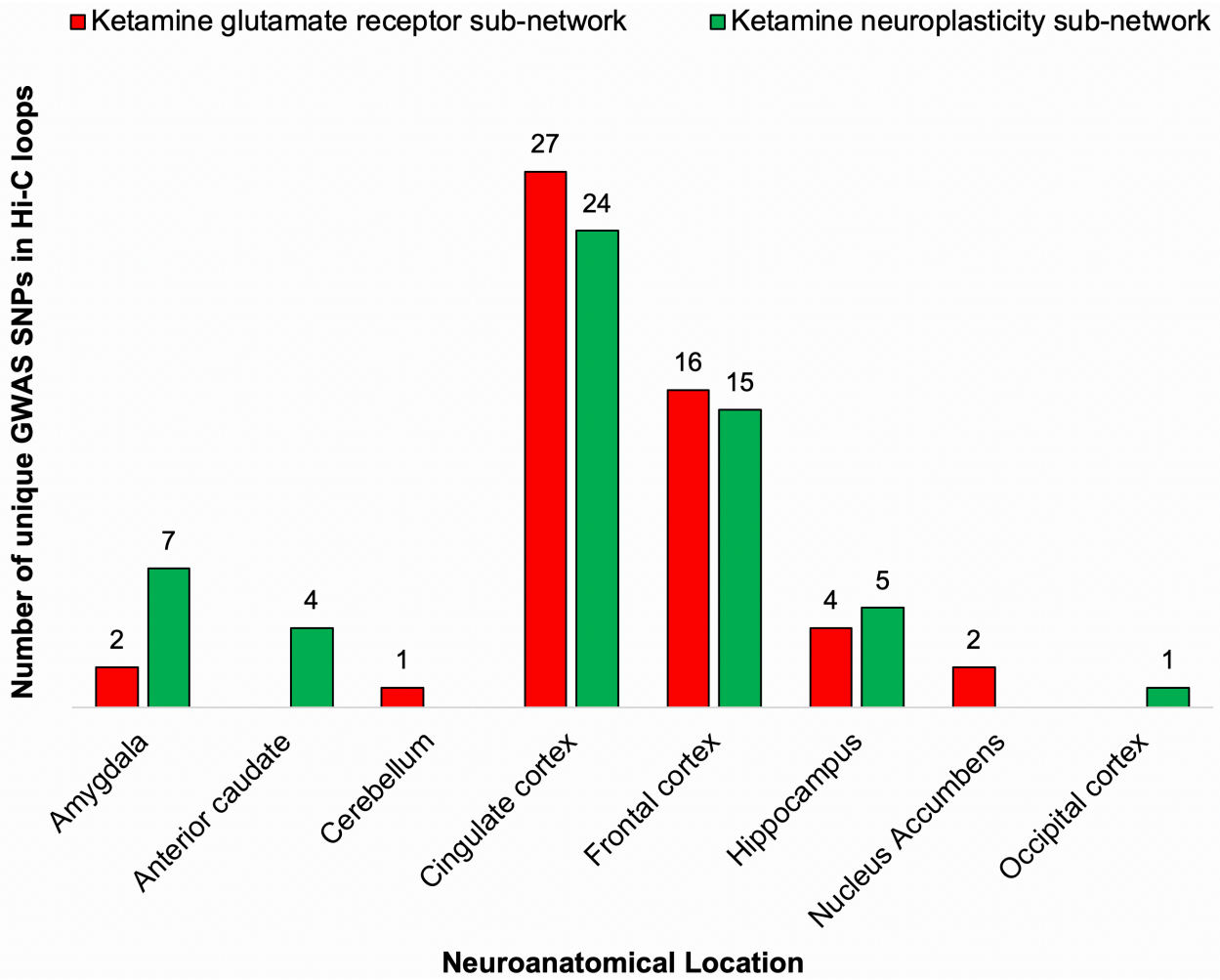

Fig. 6. The neuroanatomical distribution of 108 non-overlapping GWAS disease risk and pharmacogenomic response SNPs located within Hi-C chromatin loops in the ketamine glutamate receptor sub-network (red) and the ketamine neuroplasticity sub-network (green). Details provided in **Supplementary Tables 4 and 5**.

Evidence in support of the ketamine pharmacogenomic network identified here is demonstrable by comparing the neuroanatomical distribution of gene expression data within the ketamine sub-networks with the localization results from a consensus brain-map showing which brain regions are first impacted by ketamine obtained from 24 neuroimaging studies **(Supplementary Table 1)**. The consensus map emphasizes the anterior cingulate cortex (ACC), dorsolateral and dorsomedial prefrontal cortex (PFC), and the supplementary motor area (SMA) as consistently the first human

brain regions to be activated by the drug, indicated by the dark red spheres in **Supplementary Figure 1A**. However, other CNS regions have been reported in neuroimaging studies to be rapidly impacted by ketamine in humans following administration of the drug. These are shown in black in **Supplementary Figure 1A** but did not comprise the clear majority of brain regions reported to be first impacted by ketamine in the neuroimaging studies that we examined during our research. To serve as controls, we chose adjacent human brain regions not impacted by ketamine in the neuroimaging studies, including the corpus callosum (CC), occipital cortex (OC) and somatosensory cortex (SS). We were limited by available sources of gene expression data from postmortem human brain but did obtain reliable and non-conflicting data on 100 of the 107 genes in the ketamine network (*64, 67*). Also, the RNA sequencing (RNA-seq) results were not as well localized as the neuroimaging data, so this analysis was limited to obtaining RNA-seq data labeled as originating from anterior cingulate cortex (ACC), prefrontal cortex (PFC), corpus callosum (CC), somatosensory cortex (SS), and occipital cortex (OC). As shown in **Supplementary Figure 1B**, genes in the ketamine network are expressed at significantly higher levels in the ACC and PFC than in the neighboring CC, SS and OC, where there is no evidence that ketamine exerts rapid antidepressant effects. The ACC is part of the cingulate cortex, and the PFC is part of the frontal cortex, regions that are shown in **Table 1**, **Supplementary Figure 2**, **Supplementary Table 4** and **Supplementary Table 5**.

Publicly available *in situ* hybridization data of *GRIN2B*, *GRIN1* and *GLRB* mRNA in postmortem human brain **(Supplementary Figure 2)** (*67*) shows that expression of these three key genes located in the ketamine glutamate receptor network is widespread in the telencephalon, including amygdala, anterior caudate, anterior cingulate cortex, frontal cortex, globus pallidus,

hippocampus, prefrontal cortex, nucleus accumbens and putamen. However, there are differences in their neuroanatomical distribution. For example, *GLRB* shows circumscribed expression in layer VI of cortex, whereas *GRIN2B* and *GRIN1* are expressed in the dentate gyrus of the hippocampal formation.

Whole genome, Hi-C data mapping performed using SNPs as data probes, the probes including SNPs contained within the ketamine sub-networks and obtained from the GWAS catalog *(37)*, including those which has been significantly associated with disease risk and ketamine antidepressant response variation and dissociation (*15*). These results validated pathway analysis and demonstrated both *cis*- and *trans*-interactions with other members of the ketamine pharmacogenomic pathway within human neurons **(Figure 7, Figure 8) (Materials and Methods)**. These spatial contacts are significantly enriched for association with specific superenhancers from cingulate cortex and frontal cortex (*data not shown*). **Figure 7A** shows a whole genome plot that is the key for understanding the gene-gene interactions shown in **Figure 7B-7G**, with each individual *trans*-interaction labeled using a different color (see Key). **Figure 7B** shows Hi-C contacts between *RASGRF2*, a gene associated with synaptic plasticity and alcoholism *(70)*, with the co-localized nicotinic receptor genes *CHRNA3* and *CHRNA5* that contain SNPs significantly associated with smoking status in GWAS *(37)*. **Figure 7B** shows *trans*-interactions between the *ROBO2* gene, which contains a number of SNPs associated with both unipolar depression and dissociative and antidepressant responses to ketamine in GWAS *(15,37)*, and both the *GRIN2B* gene and the *ATF7IP* gene. The *ATF7IP* gene encodes a chromatin remodeling protein responsible for HUSH-mediated heterochromatin formation and gene silencing as part of the stabilization of the SETDB1 complex, required for methylation of histone 3 lysine 9 (H3K9me3)

during neuronal differentiation *(71)*. The *TCF4* gene, encodes a transcription factor that regulates neuronal differentiation *(15, 37)*, and harbors multiple GWAS SNPs significantly associated with recurrent depression **(Supplementary Table 4)**.

Figure 7D demonstrates a spatial contact between *TCF4* and the *GRM5* gene, which encodes a member of the glutamate metabotropic receptor family and contains enhancers significantly associated with depression in GWAS **(Supplementary Table 4)** *(37)*. **Figure 7E** shows a Hi-C map of interactions between *CACNA1C* and the *GRIN2A* and the ATF7IP2 genes. In **Figure 7C**, Hi-C spatial contacts obtained from human glutamatergic neurons shows *trans*-interactions between the *CAMK2A* gene located on chromosome 5 with the genes *GRIN1* and *ANAPC2* located on chromosome 9. The ANAPC2 protein is part of a complex that controls the formation of synaptic vesicle clustering at the active zone to the presynaptic membrane in postmitotic neurons, and this complex also degrades NEUROD2 as a primary component of pre-synaptic differentiation during neuronal differentiation *(72)*. **Figure 7G** shows spatial contacts in neurons between the *DRD2* gene and the *RHOA* gene, which encodes a signaling protein that regulates the cytoskeleton during synaptic transmission in neurons *(73)*.

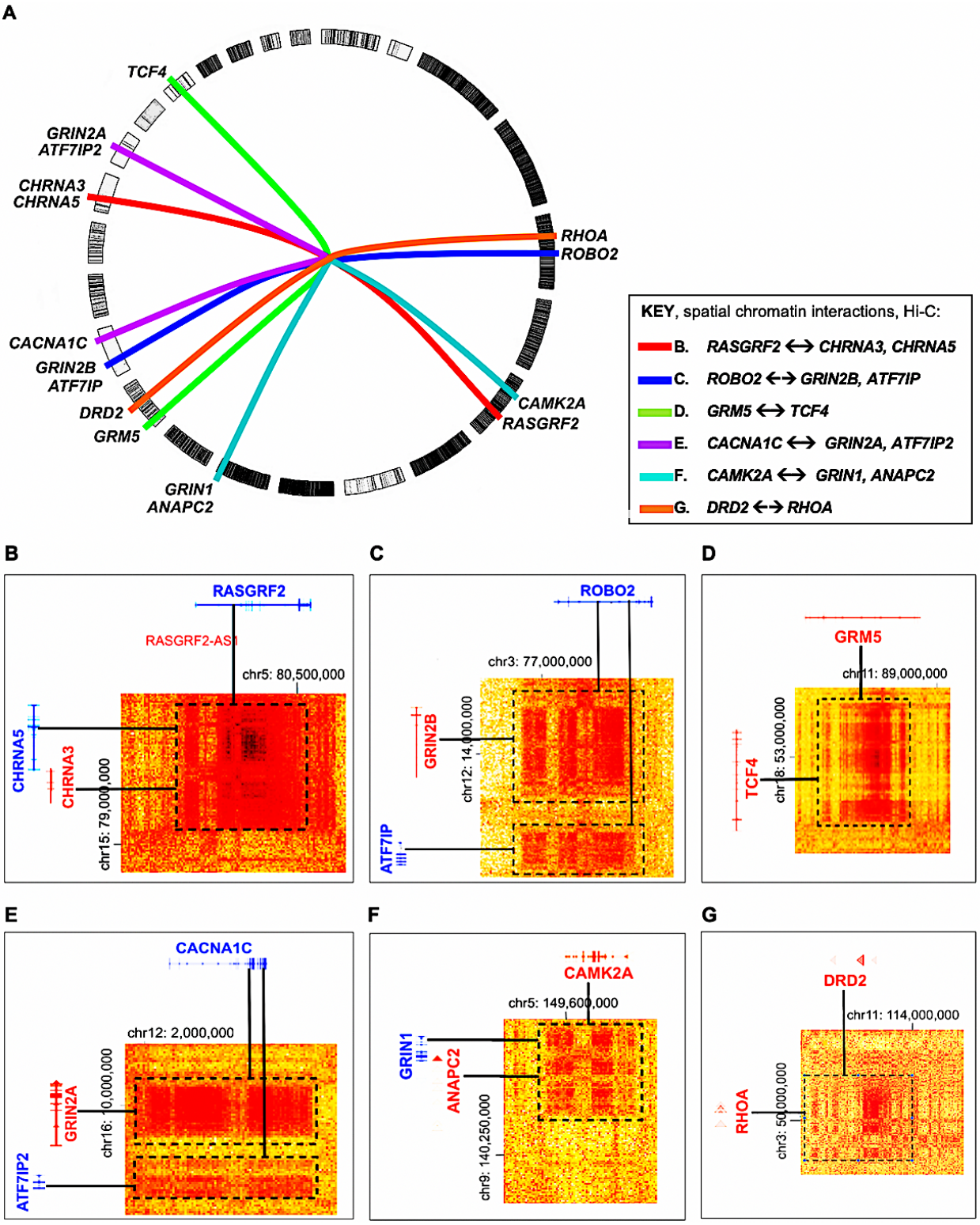

Fig. 7. Example of the *trans*-interactions of ketamine pharmacogenomic network SNPs. The intensity heat maps demonstrate individual spatial Hi-C contacts between genes in human neurons, including **(A)** *CACNA1C* and *GRIN2A* (blue line); **(C)** *RASGRF2* and *CHRNA3 CHRNA5* (orange line); **(D)** *CAMK2A* and *GRIN1, ANPAC2* (red line); **(E)** *DRD2* and *RHOA* (light blue line); **(F)**

GRM5 and *TCF4* (purple line); (G) *ROBO2* and *GRIN2B, ATF7IP* (green line); **(B)** Whole genome plot serves as key showing individual gene-gene interactions by color with the corresponding colored line located next to letters in Figure 7A, C-G. Images from Hi-C data visualization using the HiGlass software *(74)*, and coordinates are based on human genome build hg19 of the UCSC browser (*75*).

Figure 8 compares the local *cis*-interactions and organization of the loci containing the *GRIN2A* and *GRIN2B* genes in human glutamatergic neurons. In both cases, related genes are organized as triplets on different chromosomes, with the *GRIN2A*, *ATF7IP2* and *EMP2* genes on chromosome 16, and the *GRIN2B*, *ATFIP* and *EMP1* genes on chromosome 12. It is not known whether the co-localization of these 3 related genes is a coincidental, possibly a consequence of a conserved genomic duplication occurring during evolution and/or functional relatedness. **Figure 8** shows putative chromatin loops (magnified circles).

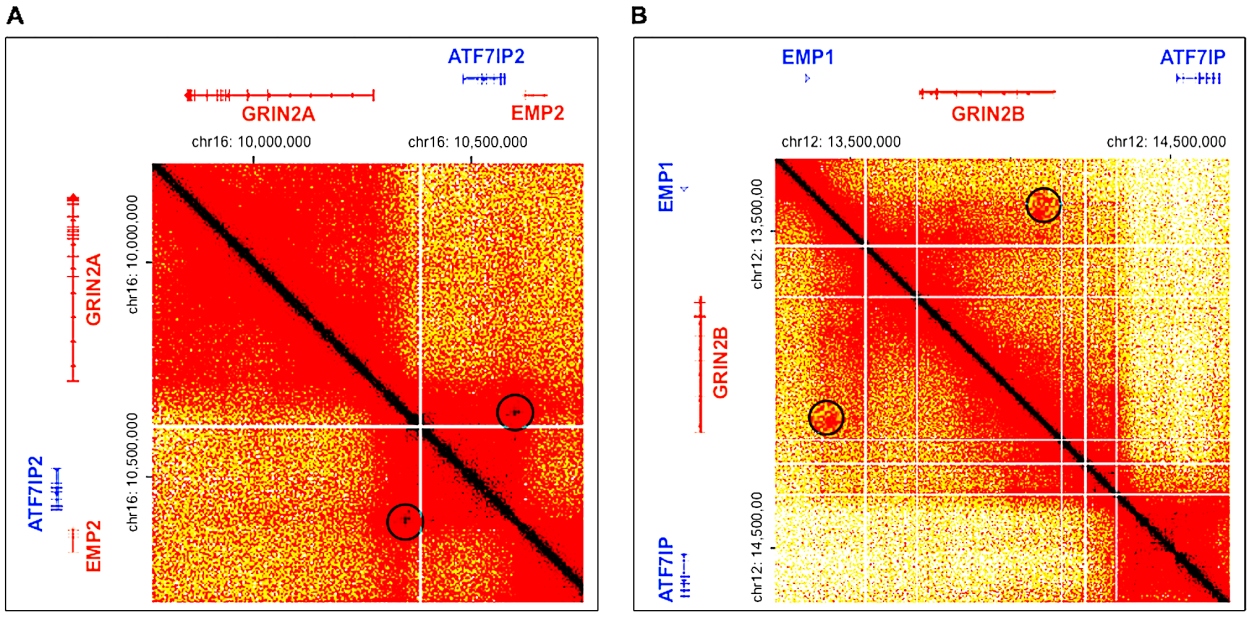

Fig. 8. Organization of the Hi-C loci containing the glutamate receptor genes *GRIN2A* and *GRIN2B* in human glutamatergic neurons. **(A)** Hi-C matrix showing the co-localized genes *GRIN2A*, *ATF7IP2* and *EMP2* **(B)** Hi-C matrix showing the co-localized genes *GRIN2B*, *ATF7IP* and *EMP1*. Circles indicate possible loop domains magnified by 2X. Images from Hi-C data visualization using the HiGlass software *(74)*, and coordinates are based on human genome build hg19 of the UCSC browser (*75*).

Discussion

The ketamine pharmacogenomic sub-networks

We have identified a ketamine pharmacogenomic network in the human brain using multi-scale biological data analysis. Our approach used multiple, reinforcing data sources and algorithms, as well as results spanning different levels of resolution, ranging from disease risk genotype-phenotype associations obtained from GWAS to functional neuroimaging of rapid antidepressant response in the human brain following ketamine administration. Special emphasis has been placed on discretization of the enhancer interactome and chromatin interactions in the context of pharmacogenomic efficacy and adverse events. Results from all of the methods applied at different scales of resolution produced consistent findings, demonstrating that this novel strategy provides a useful application for data-driven bioinformatics discovery of psychotropic drug mechanisms for future applications **(Figure 1)**. The research reported here also provides an *in-silico* design framework for subsequent study of pharmacogenomic networks in other therapeutic categories.

This research emphasizes the role of the regulatory genome, including enhancer and superenhancer-based interactomes, as an approach that provides insight into pharmacogenomic network mechanisms (*22-25*). It differs from pathway modeling methods in which altered protein folding based on missense codon variants and fixed signaling pathways serve as the foundation for the interpretation of the molecular substrate of ketamine response in humans. For example, we found no evidence for the inclusion of SNPs within proposed key signaling pathways in the ketamine network such as *AKT1, MTOR*, or *ERK1,* or participation of the inflammasome in this network (NLRP3 pathway) (*10, 17, 76, 77*). Although we do not find inflammatory genes in this ketamine network, the drug has shown promise as an investigational therapy for some

inflammatory disorders *(8)*. We did find evidence supporting the inclusion of the pharmacokinetic genes *CYP2B6* and *CYP3A4,* in addition to *ESR1* and *GRIA1, GRIA4* within the ketamine network in human brain consistent with recent studies (*12, 78*), although more study is needed to show how proteins encoded by these genes in the brain contribute to ketamine response in humans.

One possible limitation of this research is that it relies, in part, on public and commercial databases that may contain erroneous information including uncorrected confirmation bias in published literature, deprecated primary source material, and results obtained using flawed statistical methods and/or methods based on spurious assumptions. To mitigate error associated with reliance on a single data type, the approach in this study used multiple, related data sources and algorithms, spanning different levels of resolution ranging from disease risk genotype-phenotype associations obtained from GWAS to functional neuroimaging of rapid antidepressant response in the human brain following ketamine administration. Similar methods have been used to combine results from GWAS and neuroimaging data *(79)*.

The three-composite ketamine pharmacogenomic sub-networks

This research suggests that a different pharmacogenomic sub-network may mediate antidepressant effects and the dissociative and psychotomimetic effects of ketamine. Thus, the function of one sub-network is characterized by neurogenesis and neuroplasticity, as previously shown as the mechanism of action for other antidepressant medications (*9, 80, 81*). It is tempting to speculate that while ketamine may not directly cause neurogenesis in its role as an antidepressant in human brain, it may stimulate neurogenic transcription leading to renewal of intrinsic self-efficacy, a personality trait often lost in depression (*82*). In contrast, the sub-network containing genes that encode glutamate receptor proteins such as GRIN, GRIN3A and

GRIN2B not only contains the largest number of genes, but SNPs within enhancers of this sub-network have been significantly associated with dissociative disorders such as schizophrenia and bipolar disorder, and postoperative delirium, vomiting, and nausea adverse events associated with ketamine administration. Finally, enhancer SNPs in the glutamate receptor sub-network versus the neuroplasticity sub-network stratify by ketamine efficacy with reduced dissociation versus increased dissociation in response to ketamine, respectively (*15*).

The ketamine pharmacogenomic network is preferentially localized in the anterior limb of the behavioral antidepressant connectivity network, including cingulate cortex and frontal cortex in the human brain. This connectivity network was confirmed using an array of different data types, including enhancer, superenhancer, eQTL and Hi-C scoring of chromatin loops for annotation of GWAS SNPs, expression mapping, functional neuroimaging studies, and examination of the *cis*- and *trans*-interactions of ketamine pharmacogenomic SNPs.

There is a need to better understand mechanisms through which ketamine and its analogues act in the human central nervous system and to uncouple the psychotomimetic adverse effects of this emerging class of promising therapeutics from mechanisms that mediate antidepressant action. Ketamine's action as an anesthetic, analgesic and sedative may be a consequence of the partial antagonism of NMDAR-mediated pain transmission, blocking central sensitization of ascending pain afferents from the dorsal horn. Thus, through dissociation, the patient no longer pays attention to ascending pain stimuli, detached from the conscious mind, in a dreamlike state often accompanied by memory impairment (*83, 84*).

Genotype-phenotype annotation of different ketamine sub-networks

One challenge is to understand why certain phenotypes cluster within a specific ketamine pharmacogenomic sub-network. In the glutamate receptor sub-network of the larger ketamine pharmacogenomic network, significant genotype-phenotype associations that include smoking impacting the same genes as schizophrenia **(Table 1A and Supplementary Table 4)**. In the ketamine neuroplasticity sub-network, significant enhancer annotations included unipolar depression, depressive symptoms and alcoholism. This lends credence to our hypothesis that mutational disruption of the enhancer interactome within a drug network may provide insight into pharmacogenomic response stratification.

There is substantial evidence that patients diagnosed with schizophrenia are more likely to be heavy smokers than are healthy controls (*85-87*) but cause and effect are not understood. Emerging research demonstrates that nicotine induces *CYP2B6* gene expression by two to three orders of magnitude in the human brain but not in the human liver (*14*). Because the cytochrome P450 family 2 sub-member 6 enzyme encoded by the *CYP2B6* gene is rate-limiting in the metabolism of ketamine and its enantiomers (*88*), patients suffering from one of the spectrum of dissociative disorders related to schizophrenia may use nicotine for self-medication (*85*); however this hypothesis remains speculative. While exon variants in the *CYP2B6* gene may differentially alter splicing but not protein structure or function (*89*), mutations that alter *CYP2B6* mRNA splicing in the human brain contribute significantly to ketamine response variation in humans (*90, 91*). Previous research and results from this study show that estrogen regulation of *CYP2B6* gene expression can modulate differential response to ketamine in females

(biological sex) **(Figure 5)** (*92*). These results indicate that dose optimization is critically dependent on a patient's endogenous drug profile, biological sex, and age *(12, 91, 92)*.

Translation to clinical practice

These results support the conclusion that variation in genomic regulatory networks can be translated into actionable drug selection and dose optimization in patients. This study demonstrates the potential of multi-scale biological data analysis for the *in-silico* prediction of drug response and serious adverse event profiles in patients based on normal variation in the non-coding enhancer interactome and the discretization of drug-disease networks based on common genotype-phenotype associations. Thus, the antidepressant and dissociative effects of ketamine and related glutamatergic modulators, including dextromethorphan, D-cycloserine, raspastinel and sarcosine, may be uncoupled based on the patient's genetic risk profile. In this manner, knowledge of the subordinate mechanistic sub-networks of ketamine and its enantiomers explain previously unrecognized mechanisms of action of this drug class, identifying additional targets for drug repurposing. This strategy also suggests possible clinically relevant indications for ketamine that extend beyond depression, surgical anesthesia, sedation, and acute analgesia. These include psychiatric and also stress-related disorders defined by similar mechanisms of neural injury and repair, including posttraumatic stress disorder, bipolar 1 disorder, fibromyalgia, peripheral neuropathy, inflammatory bowel disease, and global chronic pain. The clinical utility of this approach requires confirmation in preclinical and clinical studies.

Materials and Methods

Selection of ketamine-response genes

The ketamine response workflow is based on the pharmacoepigenomics informatics pipeline (PIP) *(22-25)*. Input genes to the data analysis pipeline first included those genes that encode proteins and constituents of macromolecular protein complexes obtained from past studies of the binding affinity of (*R, S*)-ketamine, *R*-ketamine and *S*-ketamine performed in microsomal and tissue preparations in rodents and humans. Genes were selected based on whether their protein products, either alone or as part of a larger complex, bound ketamine enantiomers at high affinity ranging from 0.1 – 100 μM**.** To identify proteins and protein complexes, we used a search string from January 1975- October 2019 that included a Boolean search string with the words, "ketamine"", "*(RS)*-ketamine", "*(R)*-ketamine", "*(S)*-ketamine", "binding affinity", "K_i" and "IC_{50}", "brain", and "microsomes" – this search string produced 18 publications **(Supplementary Table 1)**. This gene set included *CACNA1C, CHRM2, CHRNA3, CHRNA5, CHRNA7, CNR1, DRD2*, *ESR1, GLRB, GRIA1, GRIA4, GRIN1, GRIN2A, GRIN2B, GRIN2C, GRIN2D, GRIN3A, GRIN3B, GRM5, HCN1, HTR1A, HTR1B, HTR2A, HTR3A, OPRK1, OPRM1, SIGMAR1, SLC6A2 and SLC6A3* **(**see also **Supplementary Table 3.)**

Further inputs identified candidate pharmacodynamic and pharmacokinetic genes obtained from published literature and drug databases, including DrugBank *(93)*, Ingenuity Pathway Analysis™ (IPA™; Qiagen GmBH) *(32),* the Kyoto Encyclopedia of Genes and Genomes (KEGG) *(35)*, and DrugCentral *(94).* This subset included genes not listed in the above set of candidate genes, but excluded pharmacodynamic targets that had not been shown to bind ketamine and its enantiomers at high affinity. This subset included genes and regulatory RNAs: *ACHE, AKT1, ANAPC2, AR,*

ARC, ARNT, ASCL1, ATF7IP, ATF7IP2, ATP1A1, BDNF, BDNF-AS, BORCS7, CACNA1C, CACNB1, CACNB2, CACNG2, CAMK2A, CDKN1A, CREM, CUX2, CYP2A6, CYP2B6, CYP2C9, CYPC19, CYP3A4, DCC, DLG3, DLG4, DNMT1, DOCK10, EDN2, EEF2, EEF2K, EHTM1, ENSG00000225960, ENSG00000251574, ERK1, ERK2, ESR1, FMR1, GABBR1, GABRA2, GABRA5, GAD1, GDAP1L1, GFAP, GLRA1, GLRA2, GRIP1, HDAC5, HK1, HMOX1, HOMER1, KLF6, LAMTOR1, LEP, LIN7C, MAPK1, MAPK8, MBD1, MEF2D, MPHOSPH8, MTOR, MTRNR2L2, MYO6, MYT1L, NMB, NCAM1, NEUROD1, NEUROD2, NLRP3, NMB, NOS1, NOS2, NOS3, NQO1, NR4A1, NSMF, NTRK2, PGBD1, PTGS2, PVALB, RAC1, RASGRF2, RHOA, ROBO2, RPTOR, SEC11A, SEMA3A, SETDB1, SHANK1, SHANK2, SHANK3, SLC6A9, SLC22A15, SLIT1, SLIT2, SNAP25, SYN1, SYN2, SYT3, TASOR, TBR1, TBX21, TCERG1, TCF4, TMPRSS5, TMPRRS6, TOGARAM2, TRIM26, TRIM28, ZNF274, ZNF592 and *ZNF717.*

Criteria for further selection of candidate genes was 2-fold. First, we determined whether the gene or regulatory RNA was expressed in human brain regions rapidly activated by ketamine enantiomers as determined by functional neuroimaging. The neuroanatomical distribution of the expression of genes in the ketamine network and its sub-networks were matched to a consensus map of brain regions rapidly activated by ketamine, based on the results of 24 neuroimaging studies in healthy controls and patients diagnosed with unipolar and bipolar depression **(Supplementary Table 1)**. Second, we assessed whether this gene set formed a significantly interconnected pathway in human brain using neural cell- and tissue-specific filtering. Results were generated using IPA™ (Qiagen GmBH) and verified using the STRING protein-protein interaction network database *(33)*. Independent software applications for the *post-hoc* bioinformatics analysis included enrichment

analysis using Gene Ontology's Panther web-based portal *(34)* and the gene expression module of IPA™ to determine disease risk based on published literature *(32)*.

Gene set optimization, pathway analysis and significant upstream molecular regulators

Following reconstruction of the larger ketamine spatial network, it was deconstructed into its associative mechanistic sub-networks using an executable gene set optimization engine that iteratively compares gene function with efficacy, adverse events and other known features associated with ketamine response **(Figure 9)**. The iterative mechanistic sub-network profiler comprises executable code that iteratively re-organizes interconnected gene sets within the drug spatial network until the most significant associations with the various mechanisms of action of the psychotropic drug are reached, based on multiple databases including Gene Ontology *(34)*.

Independent pathway analysis software applications were used for the *post-hoc* bioinformatics analysis including the gene expression module of IPA™ *(32)* and KEGG *(35)* to determine disease risk, based on results extracted from the published literature. In addition, ketamine sub-network genes were annotated using data from the EBI-NHGRI GWAS catalog *(37)* to assess the potential of sub-network function through the identification of significant SNP-trait associations for every gene in each sub-network. We hypothesized that mutations within gene subsets that comprise each sub-network, as exemplified by SNP-trait associations from GWAS, were determined to be relevant to ketamine efficacy and adverse events and, as such, might provide further insight into the normal, unimpaired function of the various sub-networks.

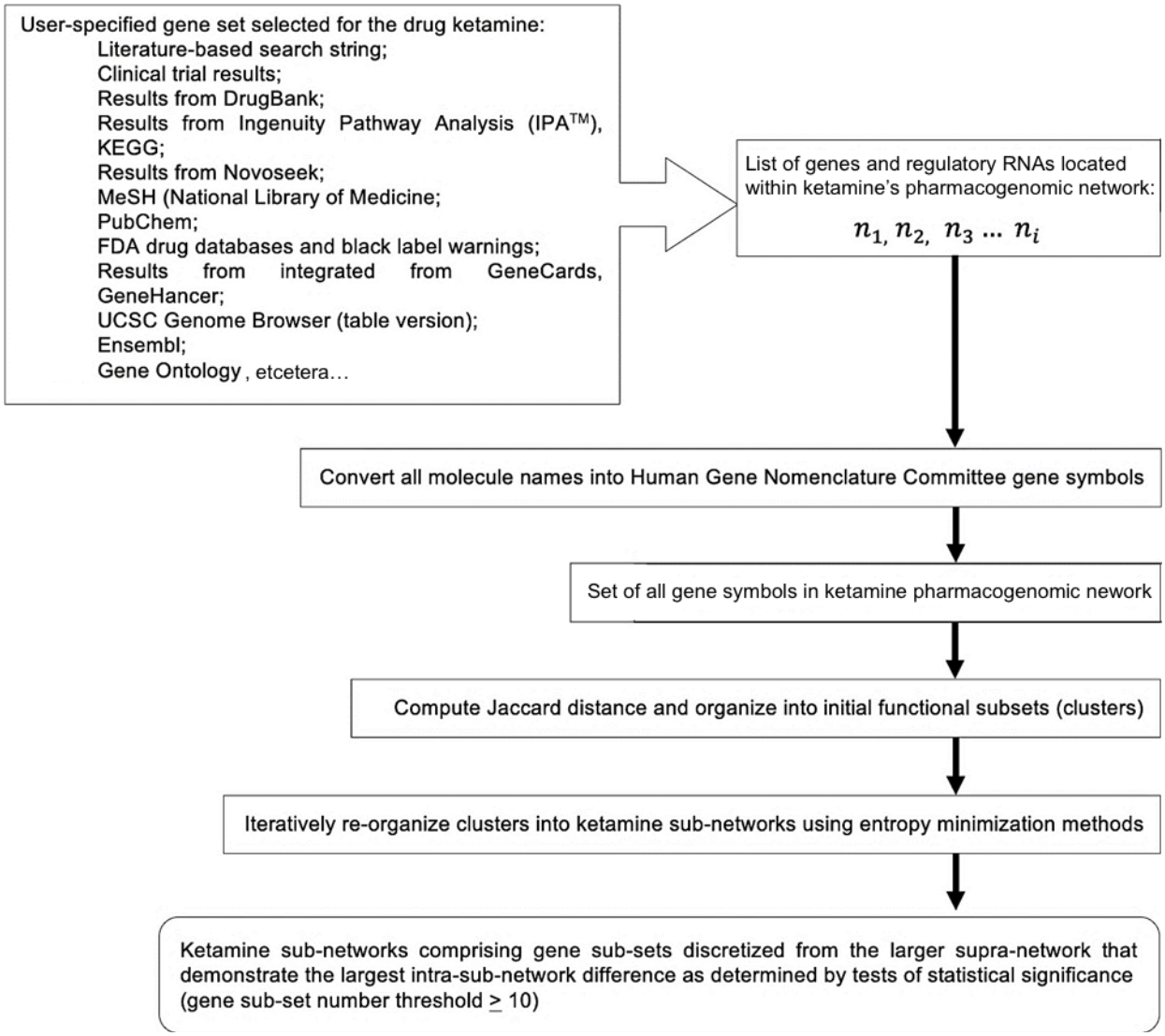

Figure 9. Iterative gene set optimization workflow. This iterative gene set optimization executable differs from gene set enrichment methods, by not only combining different mathematical methods, but also not acting in a hierarchal manner ranking genes as in threshold-dependent methods until the output, and this iterative gene set optimization does not rely on comparisons of experimental results, such as in whole-distribution tests. Instead, the iterative gene set optimization groups genes or long noncoding RNAs using the Jaccard distance to first measure the similarity between two genes or long noncoding RNAs based on the dissimilarity of user-selected terms, where the Jaccard distance is as the ratio of the size of the symmetric difference *Gene A* Δ *Gene* $B = A \cap B - A \cup B$ to the union. This is extensible into clusters of related dissimilar gene names. A drug network server then automatically sorts these sets, or using user-defined numbers of clusters, into subsets of clustered subsets of functionally related genes using a minimal entropy sorting algorithm, such as the COOLCAT algorithm *(94)*. Following gene subset optimization using entropy minimization, the pharmacogenomic spatial network identification system may employ manual curation to assign efficacy, adverse event or functional mechanistic sub-networks based on known attributes of the drug's mechanism of actions under consideration.

Selection of candidate ketamine response SNPs

Our pharmaco-informatics platform processes data with minimal human intervention to avoid in-house bias. Human SNPs were selected and processed using a revised version of the bioinformatics pipeline that has been described in detail in previous publications *(22-25)*. For the workflow used in this study, GWAS SNPs were used as reported. These SNPs included all variants from GWAS related to genes within the larger ketamine pharmacogenomic network including genes located in the composite sub-networks. These included both SNP signals significantly associated with disease risk and those associated with ketamine antidepressant response efficacy and dissociation, as well as other ketamine network and sub-network-associated SNPs from the published literature and clinical trials *(8, 37)*. The SNP filter judged candidate ketamine network SNPs for putative causality using multiple, redundant machine learning algorithms *(39-45)*. The 65,535 SNPs contained in the EBI-NHGRI GWAS catalog *(37)* were evaluated for the 110-putative ketamine-response genes and regulatory RNAs contained in our sub-networks. Phenotypes that were defined by self-reporting, such as educational attainment, mathematical ability and intelligence, were not included. Phenotypes, including insomnia and neuroticism, were also not included as there are various interpretations of these psychiatric surrogate associations. Since a plethora of GWAS SNPs associated with schizophrenia and depression were found to be primary determinants of differences between the ketamine glutamate receptor sub-network and the ketamine neuroplasticity sub-network, we undertook to provide greater clarification of these broad-spectrum phenotypes into subtypes. Phenotypes including smoking status, alcohol and substance abuse, nausea, vomiting and migraine were included based on their relevance to the psychological features of patients or the mechanisms of action of ketamine and its enantiomers. The genotype-

phenotype association annotations were examined for determination of differences between the ketamine glutamate receptor sub-network and the ketamine neuroplasticity sub-network.

Numerical scores from each algorithm are generated for each GWAS SNP and only in cases where each output scored the SNP as predicted to be causal in SK-N-SH cells and H1 cells, but not in HepG2 cells and PBMCs, were the SNPs retained for further analysis. These numerical scores for every SNP are shown in **Supplementary Table 4** and **Supplementary Table 5**. The score of every predicted causal SNP was independently tested to determine if it differed significantly from the scores generated using 10 randomly selected GWAS SNPs for all human traits at $p \leq$5E-08 listed in the EBI-NHGRI GWAS catalogue *(34)* using ANOVA. Only when the SNP met this criterion of significance, was it selected for further analysis. An example for the SNP rs12967143-G, an intragenic enhancer within the *TCF4* gene, is shown in **Figure 10**.

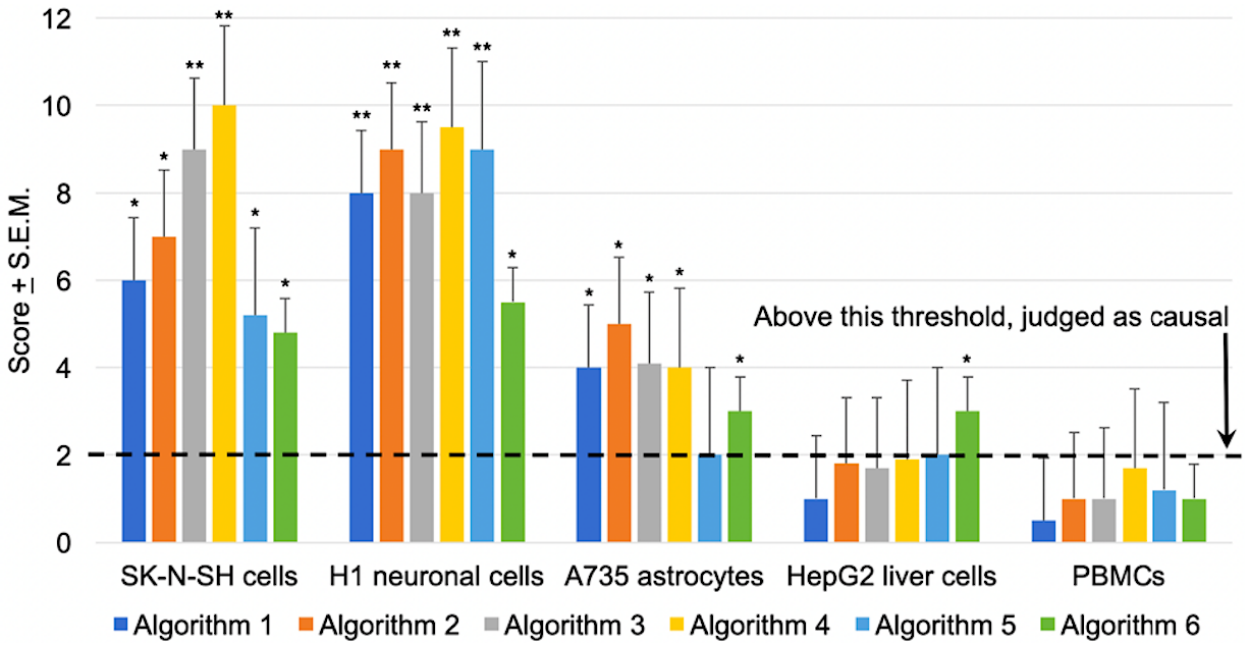

Figure 10. Results of significance testing of the SNP rs12967143-G, an intragenic enhancer located in the *TCF4* gene, versus other GWAS SNPs as described using the numerical output from the machine learning algorithms used in the analysis. *$p \leq 0.05$; ** $p \leq 0.01$.

Annotation of enhancer-promoter pairs and chromatin contacts in neural cell lines and brain

GWAS SNPs within the 2 different ketamine sub-networks were annotated by disease risk, psychiatric subtype, enhancer, promoter, superenhancer and enhancer RNA co-localization, enhancer promoter interactions determined by Hi-C chromatin interactions using public data sources. We used an advanced version of an adjustable bin mapping method (formerly called "Hi-C compiling with Genomic and Regulatory Elements and Empirical Normalization"("H-GREEN")) method in which candidate ketamine response SNPs judged as causal using machine learning were used to probe public sources of Hi-C data obtained from SK-N-SH, H1, and A735 cells. This approach was used to verify public data on the localization of enhancer-promoter pairs. The method employs non-fixed, adjustable binning analytic software, which provides much higher resolution for point-to-point mapping in squared human genome space than other methods. The adjustable bin mapping method maps ketamine SNPs to determine the distribution of TADs altered by various psychotropic drugs within the chromatin interactome and the *cis*- and *trans*-interactions of TADs containing pharmacogenomic SNPs for ketamine that were assessed in neuronal, astrocyte, hepatocyte cell lines and peripheral blood mononuclear cells.

To map genomic element contacts, this chromatin interaction method obtains a set of genomic loci and segments the set into bins of varying sizes. The method selects 2 sets of bins corresponding to the home TAD of the pharmacogenomic SNP and one of its contact TADs (e.g., a first set of bins corresponding to chromosome 1 and a second set of bins corresponding to chromosome 8) and places them in an n x m matrix (a squared genome area) to generate a set of bin pairs. Accordingly, the squared genome area may be of variable size and shape. In some run versions, both sets of bins are the same (e.g., each corresponding to chromosome 1). The chromatin

interaction system identifies pairs of locations corresponding to paired end reads or other spatially interacting locations with bin pairs that contain them, i.e. wherein one of the bins contains one locus and the other bin contains the other locus, using a binary search tree. Then an interaction frequency is generated for each bin pair based on the genomic element contacts within the corresponding bin pair. The interaction frequencies are normalized per the density of pairwise contacts as a function of genomic distance within each bin pair. More specifically, the density of pairwise contacts as a function of genomic distance is generated using a normalized density function.

For a bin pair containing origin and target contact TADs, the density function is integrated over the squared genome area of the bin pair to determine an expected density for the bin pair. The expected density is then compared to the actual density for the bin pair (i.e., the number of pairwise contacts within the squared genome area of the bin pair) using the statistical test of Benjamini-Hochberg false discovery rate *(96)*. These generate a collection of enriched and depleted chromatin contacts in a manner adjusted for distance (and other features as appropriate), on a local and genomewide basis. The chromatin interaction system then provides indications of the bin pairs having, for example, enriched or depleted contacts for display on a user interface. By using variable bin sizes, the chromatin interaction system enables adjustable Hi-C bin mapping, regardless of bin length.

Neuroanatomical localization of enhancer sub-networks

First, comparison was made between the expression patterns of genes within the ketamine sub-networks with a consensus heatmap of the drug's rapid antidepressant response map derived from

functional neuroimaging, as previously described **(Supplementary Figure 1)**. Second, we evaluated the 108 non-overlapping GWAS SNPs annotated for their putative regulatory function as enhancers, promoters, superenhancers and splice variants, and then used a variety of sources of Hi-C data for neuroanatomical assignment to human brain regions including the amygdala, anterior caudate, cerebellum, cingulate cortex, frontal cortex, hippocampus, nucleus accumbens and the occipital cortex from Hi-C data *(46, 61, 62, 74)*.

Whole genome, Hi-C mapping performed using disease risk and pharmacogenomic SNPs

In addition to the adjustable bin mapping method developed in our laboratory, we used a local instance of the HiGlass software for rapid identification of the *cis*- and *trans*-interactions of all of the 108 non-overlapping GWAS SNPs shown in **Supplementary Table 4** and **Supplementary Table 5** *(74)*. This client-server software converts single resolution 1D linear human genome into multi-resolution formats that can be interactively searched in Hi-C from neuronal cells and tissues, and other sources, for spatial chromatin contacts. This software was used to generate a set of spatial interactions for the ketamine glutamate receptor sub-network and the ketamine neuroplasticity sub-network. In excitatory human glutamate neurons, the following have both *cis*- and *trans*-interactions with all members of this gene set: *ATFIP2, CACNA1C, CACNG2, CHNRNA3, DRD2, GRIN1, GRIN2A, GRIN2B, NOS1 and SETDB1,* compared to other tissues or cell lines. In neuronal cell lines, the following genes had both *cis*- and *trans*-interactions with each other: *TCF4, DCC,* and *GRM5,* compared to other tissues or cell lines. Examples of gene pair *trans* interactions within and between the sub-networks is shown in **Figure 7**, and local *cis* interactions are shown for the *GRIN2A* and *GRIN2B* loci in **Figure 8**.

References

1. P. Cuijpers, The challenges of improving treatments for depression. *Jama* **320**, 2529-2530 (2018).
2. K. Jonkman, A. Dahan, T. van de Donk, L. Aarts, M. Niesters, M. van Velzen, Ketamine for pain [version 1; peer review: 2 approved]. *F1000Research* **6**, (2017).
3. J. F. Greden, M. B. Riba, M. G. McInnis, U. M. C. D. Center, *Treatment Resistant Depression: A Roadmap for Effective Care*. (American Psychiatric Publishing, 2011).
4. V. A. Canady, FDA panel endorses ketamine nasal spray for depression. *Mental Health Weekly* **29**, 6-7 (2019).
5. R. Machado-Vieira, G. Salvadore, N. Diazgranados, C. A. Zarate, Jr., Ketamine and the next generation of antidepressants with a rapid onset of action. *Pharmacology & therapeutics* **123**, 143-150 (2009).
6. M. J. Niciu, I. D. Henter, D. A. Luckenbaugh, C. A. Zarate, Jr., D. S. Charney, Glutamate receptor antagonists as fast-acting therapeutic alternatives for the treatment of depression: ketamine and other compounds. *Annual review of pharmacology and toxicology* **54**, 119-139 (2014).
7. E. J. Daly, J. B. Singh, M. Fedgchin, K. Cooper, P. Lim, R. C. Shelton, M. E. Thase, A. Winokur, L. Van Nueten, H. Manji, W. C. Drevets, Efficacy and safety of intranasal esketamine adjunctive to oral antidepressant therapy in treatment-resistant depression: A randomized clinical trial. *JAMA psychiatry* **75**, 139-148 (2018).
8. P. Zanos, R. Moaddel, P. J. Morris, L. M. Riggs, J. N. Highland, P. Georgiou, E. F. R. Pereira, E. X. Albuquerque, C. J. Thomas, C. A. Zarate, Jr., T. D. Gould, Ketamine and ketamine metabolite pharmacology: Insights into therapeutic mechanisms. *Pharmacological reviews* **70**, 621-660 (2018).
9. R. N. Moda-Sava, M. H. Murdock, P. K. Parekh, R. N. Fetcho, B. S. Huang, T. N. Huynh, J. Witztum, D. C. Shaver, D. L. Rosenthal, E. J. Alway, K. Lopez, Y. Meng, L. Nellissen, L. Grosenick, T. A. Milner, K. Deisseroth, H. Bito, H. Kasai, C. Liston, Sustained rescue of prefrontal circuit dysfunction by antidepressant-induced spine formation. *Science* **364**, (2019).
10. J. M. Li, L. L. Liu, W. J. Su, B. Wang, T. Zhang, Y. Zhang, C. L. Jiang, Ketamine may exert antidepressant effects via suppressing NLRP3 inflammasome to upregulate AMPA receptors. *Neuropharmacology* **146**, 149-153 (2019).
11. X. Chen, S. Shu, D. A. Bayliss, HCN1 channel subunits are a molecular substrate for hypnotic actions of ketamine. *The Journal of neuroscience : the official journal of the Society for Neuroscience* **29**, 600-609 (2009).
12. M. F. Ho, C. Correia, J. N. Ingle, R. Kaddurah-Daouk, L. Wang, S. H. Kaufmann, R. M. Weinshilboum, Ketamine and ketamine metabolites as novel estrogen receptor ligands: Induction of cytochrome P450 and AMPA glutamate receptor gene expression. *Biochemical pharmacology* **152**, 279-292 (2018).
13. J. Li, F.F. Chen, X.D. Chen, C. Zhou, C. Inhibition of HCN1 channels by ketamine accounts for its antidepressant actions. *Journal of Sichuan University. Medical science edition* **45**, 888-92 (2014).
14. D. M. McMillan, R. F. Tyndale, CYP-mediated drug metabolism in the brain impacts drug response. *Pharmacology & therapeutics* **184**, 189-200 (2018).
15. W. Guo, R. Machado-Vieira, S. Mathew, J. W. Murrough, D. S. Charney, M. Grunebaum, M. A. Oquendo, B. Kadriu, N. Akula, I. Henter, P. Yuan, K. Merikangas, W. Drevets, M. Furey, J. J. Mann, F. J. McMahon, C. A. Zarate, Jr., Y. Y. Shugart, Exploratory genome-wide association analysis of response to ketamine and a polygenic analysis of response to scopolamine in depression. *Translational psychiatry* **8**, 280 (2018).
16. E. C. Sales, E. L. Heckman, T. L. Warren, C. Q. Doe, Regulation of subcellular dendritic synapse specificity by axon guidance cues. *eLife* **8**, (2019).
17. N. Li, B. Lee, R. J. Liu, M. Banasr, J. M. Dwyer, M. Iwata, X. Y. Li, G. Aghajanian, R. S. Duman, mTOR-dependent synapse formation underlies the rapid antidepressant effects of NMDA antagonists. *Science* **329**, 959-964 (2010).
18. C. S. Jernigan, D. B. Goswami, M. C. Austin, A. H. Iyo, A. Chandran, C. A. Stockmeier, B. Karolewicz, The mTOR signaling pathway in the prefrontal cortex is compromised in major depressive disorder. *Progress in neuro-psychopharmacology & biological psychiatry* **35**, 1774-1779 (2011).
19. G. Laje, N. Lally, D. Mathews, N. Brutsche, A. Chemerinski, N. Akula, B. Kelmendi, A. Simen, F. J. McMahon, G. Sanacora, C. Zarate, Jr., Brain-derived neurotrophic factor Val66Met polymorphism and antidepressant efficacy of ketamine in depressed patients. *Biological psychiatry* **72**, e27-28 (2012).

20. G. M. Murphy, Jr., J. E. Sarginson, H. S. Ryan, R. O'Hara, A. F. Schatzberg, L. C. Lazzeroni, BDNF and CREB1 genetic variants interact to affect antidepressant treatment outcomes in geriatric depression. *Pharmacogenetics and genomics* **23**, 301-313 (2013).
21. R. S. Duman, N. Li, R. J. Liu, V. Duric, G. Aghajanian, Signaling pathways underlying the rapid antidepressant actions of ketamine. *Neuropharmacology* **62**, 35-41 (2012).
22. G. A. Higgins, A. M. Williams, A. S. Ade, H. B. Alam, B. D. Athey, Druggable transcriptional networks in the human neurogenic epigenome. *Pharmacological reviews* **71**, 520-538 (2019).
23. G. A. Higgins, A. Allyn-Feuer, B. D. Athey, Epigenomic mapping and effect sizes of noncoding variants associated with psychotropic drug response. *Pharmacogenomics* **16**, 1565-1583 (2015).
24. G. A. Higgins, A. Allyn-Feuer, E. Barbour, B. D. Athey, A glutamatergic network mediates lithium response in bipolar disorder as defined by epigenome pathway analysis. *Pharmacogenomics* **16**, 1547-1563 (2015).
25. A. A. Kalinin, G. A. Higgins, N. Reamaroon, S. Soroushmehr, A. Allyn-Feuer, I. D. Dinov, K. Najarian, B. D. Athey, Deep learning in pharmacogenomics: from gene regulation to patient stratification. *Pharmacogenomics* **19**, 629-650 (2018).
26. S. Dong, A. P. Boyle, Predicting functional variants in enhancer and promoter elements using RegulomeDB. *Human mutation* **40**, 1292-1298 (2019).
27. M. T. Maurano, R. Humbert, E. Rynes, R. E. Thurman, E. Haugen, H. Wang, A. P. Reynolds, R. Sandstrom, H. Qu, J. Brody, A. Shafer, F. Neri, K. Lee, T. Kutyavin, S. Stehling-Sun, A. K. Johnson, T. K. Canfield, E. Giste, M. Diegel, D. Bates, R. S. Hansen, S. Neph, P. J. Sabo, S. Heimfeld, A. Raubitschek, S. Ziegler, C. Cotsapas, N. Sotoodehnia, I. Glass, S. R. Sunyaev, R. Kaul, J. A. Stamatoyannopoulos, Systematic localization of common disease-associated variation in regulatory DNA. *Science* **337**, 1190-1195 (2012).
28. S. Onengut-Gumuscu, W. M. Chen, O. Burren, N. J. Cooper, A. R. Quinlan, J. C. Mychaleckyj, E. Farber, J. K. Bonnie, M. Szpak, E. Schofield, P. Achuthan, H. Guo, M. D. Fortune, H. Stevens, N. M. Walker, L. D. Ward, A. Kundaje, M. Kellis, M. J. Daly, J. C. Barrett, J. D. Cooper, P. Deloukas, J. A. Todd, C. Wallace, P. Concannon, S. S. Rich, Fine mapping of type 1 diabetes susceptibility loci and evidence for colocalization of causal variants with lymphoid gene enhancers. *Nature genetics* **47**, 381-386 (2015).
29. Y. G. Tak, P. J. Farnham, Making sense of GWAS: using epigenomics and genome engineering to understand the functional relevance of SNPs in non-coding regions of the human genome. *Epigenetics & chromatin* **8**, 57 (2015).
30. S. C. Parker, M. L. Stitzel, D. L. Taylor, J. M. Orozco, M. R. Erdos, J. A. Akiyama, K. L. van Bueren, P. S. Chines, N. Narisu, B. L. Black, A. Visel, L. A. Pennacchio, F. S. Collins, Chromatin stretch enhancer states drive cell-specific gene regulation and harbor human disease risk variants. *Proceedings of the National Academy of Sciences of the United States of America* **110**, 17921-17926 (2013).
31. P. Collas, T. M. Liyakat Ali, A. Brunet, T. Germier, Finding friends in the crowd: Three-dimensional cliques of topological genomic domains. *Frontiers in genetics* **10**, 602 (2019).
32. A. Kramer, J. Green, J. Pollard, Jr., S. Tugendreich, Causal analysis approaches in Ingenuity Pathway Analysis. *Bioinformatics (Oxford, England)* **30**, 523-530 (2014).
33. D. Szklarczyk, A. L. Gable, D. Lyon, A. Junge, S. Wyder, J. Huerta-Cepas, M. Simonovic, N. T. Doncheva, J. H. Morris, P. Bork, L. J. Jensen, C. V. Mering, STRING v11: protein-protein association networks with increased coverage, supporting functional discovery in genome-wide experimental datasets. *Nucleic Acids Res* **47**, D607-d613 (2019).
34. H. Mi, A. Muruganujan, D. Ebert, X. Huang, P. D. Thomas, PANTHER version 14: more genomes, a new PANTHER GO-slim and improvements in enrichment analysis tools. *Nucleic Acids Res* **47**, D419-d426 (2019).
35. M. Kanehisa, Y. Sato, M. Furumichi, K. Morishima, M. Tanabe, New approach for understanding genome variations in KEGG. *Nucleic Acids Res* **47**, D590-d595 (2019).
36. J. R. Dixon, S. Selvaraj, F. Yue, A. Kim, Y. Li, Y. Shen, M. Hu, J. S. Liu, B. Ren, Topological domains in mammalian genomes identified by analysis of chromatin interactions. *Nature* **485**, 376-380 (2012).
37. A. Buniello, J. A. L. MacArthur, M. Cerezo, L. W. Harris, J. Hayhurst, C. Malangone, A. McMahon, J. Morales, E. Mountjoy, E. Sollis, D. Suveges, O. Vrousgou, P. L. Whetzel, R. Amode, J. A. Guillen, H. S. Riat, S. J. Trevanion, P. Hall, H. Junkins, P. Flicek, T. Burdett, L. A. Hindorff, F. Cunningham, H. Parkinson, The NHGRI-EBI GWAS Catalog of published genome-wide association studies, targeted arrays and summary statistics 2019. *Nucleic Acids Res* **47**, D1005-d1012 (2019).
38. G. Stelzer, N. Rosen, I. Plaschkes, S. Zimmerman, M. Twik, S. Fishilevich, T. I. Stein, R. Nudel, I. Lieder, Y. Mazor, S. Kaplan, D. Dahary, D. Warshawsky, Y. Guan-Golan, A. Kohn, N. Rappaport, M. Safran, D.

Lancet, The GeneCards Suite: From Gene Data Mining to Disease Genome Sequence Analyses. *Current protocols in bioinformatics* **54**, 1.30.31-31.30.33 (2016).

39. B. Yang, F. Liu, C. Ren, Z. Ouyang, Z. Xie, X. Bo, W. Shu, BiRen: predicting enhancers with a deep-learning-based model using the DNA sequence alone. *Bioinformatics (Oxford, England)* **33**, 1930-1936 (2017).
40. D. Lee, D. U. Gorkin, M. Baker, B. J. Strober, A. L. Asoni, A. S. McCallion, M. A. Beer, A method to predict the impact of regulatory variants from DNA sequence. *Nature genetics* **47**, 955-961 (2015).
41. S. Li, R. V. Alvarez, R. Sharan, D. Landsman, I. Ovcharenko, Quantifying deleterious effects of regulatory variants. *Nucleic Acids Res* **45**, 2307-2317 (2017).
42. D. Quang, X. Xie, DanQ: a hybrid convolutional and recurrent deep neural network for quantifying the function of DNA sequences. *Nucleic Acids Res* **44**, e107 (2016).
43. D. R. Kelley, J. Snoek, J. L. Rinn, Basset: learning the regulatory code of the accessible genome with deep convolutional neural networks. *Genome research* **26**, 990-999 (2016).
44. B. Han, M. Park, X. W. Chen, A Markov blanket-based method for detecting causal SNPs in GWAS. *BMC bioinformatics* **11 Suppl 3**, S5 (2010).
45. G. E. Hoffman, J. Bendl, K. Girdhar, E. E. Schadt, P. Roussos, Functional interpretation of genetic variants using deep learning predicts impact on chromatin accessibility and histone modification. *Nucleic Acids Res*, (2019).
46. A. Allyn-Feuer, Thesis, University of Michigan, Ann Arbor, Michigan 48109 U.S.A. (2018).
47. L. Wright, S. M. Tobias, A. Hickman, *Coding and documentation compliance for the ICD and DSM*. (Routledge New York, 2017).
48. N. Rappaport, M. Twik, I. Plaschkes, R. Nudel, T. Iny Stein, J. Levitt, M. Gershoni, C. P. Morrey, M. Safran, D. Lancet, MalaCards: an amalgamated human disease compendium with diverse clinical and genetic annotation and structured search. *Nucleic Acids Res* **45**, D877-d887 (2017).
49. A. Khan, X. Zhang, dbSUPER: a database of super-enhancers in mouse and human genome. *Nucleic Acids Res* **44**, D164-171 (2016).
50. Y. Wei, S. Zhang, S. Shang, B. Zhang, S. Li, X. Wang, F. Wang, J. Su, Q. Wu, H. Liu, Y. Zhang, SEA: a super-enhancer archive. *Nucleic Acids Res* **44**, D172-179 (2016).
51. S. Fishilevich, R. Nudel, N. Rappaport, R. Hadar, I. Plaschkes, T. Iny Stein, N. Rosen, A. Kohn, M. Twik, M. Safran, D. Lancet, D. Cohen, GeneHancer: genome-wide integration of enhancers and target genes in GeneCards. *Database : the journal of biological databases and curation* **2017**, (2017).
52. R. Dreos, G. Ambrosini, R. Groux, R. Cavin Perier, P. Bucher, The eukaryotic promoter database in its 30th year: focus on non-vertebrate organisms. *Nucleic Acids Res* **45**, D51-d55 (2017).
53. R. Umarov, H. Kuwahara, Y. Li, X. Gao, V. Solovyev, Promoter analysis and prediction in the human genome using sequence-based deep learning models. *Bioinformatics (Oxford, England)* **35**, 2730-2737 (2019).
54. P. Belokopytova, E. Mozheiko, M. Nuriddinov, D. Fishman, V. Fishman, Quantitative prediction of enhancer-promoter interactions. *bioRxiv*, 541011 (2019).
55. Y. Murakawa, M. Yoshihara, H. Kawaji, M. Nishikawa, H. Zayed, H. Suzuki, C. Fantom, Y. Hayashizaki, Enhanced Identification of Transcriptional Enhancers Provides Mechanistic Insights into Diseases. *Trends in genetics : TIG* **32**, 76-88 (2016).
56. F. Cunningham, P. Achuthan, W. Akanni, J. Allen, M. R. Amode, I. M. Armean, R. Bennett, J. Bhai, K. Billis, S. Boddu, C. Cummins, C. Davidson, K. J. Dodiya, A. Gall, C. G. Giron, L. Gil, T. Grego, L. Haggerty, E. Haskell, T. Hourlier, O. G. Izuogu, S. H. Janacek, T. Juettemann, M. Kay, M. R. Laird, I. Lavidas, Z. Liu, J. E. Loveland, J. C. Marugan, T. Maurel, A. C. McMahon, B. Moore, J. Morales, J. M. Mudge, M. Nuhn, D. Ogeh, A. Parker, A. Parton, M. Patricio, A. I. Abdul Salam, B. M. Schmitt, H. Schuilenburg, D. Sheppard, H. Sparrow, E. Stapleton, M. Szuba, K. Taylor, G. Threadgold, A. Thormann, A. Vullo, B. Walts, A. Winterbottom, A. Zadissa, M. Chakiachvili, A. Frankish, S. E. Hunt, M. Kostadima, N. Langridge, F. J. Martin, M. Muffato, E. Perry, M. Ruffier, D. M. Staines, S. J. Trevanion, B. L. Aken, A. D. Yates, D. R. Zerbino, P. Flicek, Ensembl 2019. *Nucleic Acids Res* **47**, D745-d751 (2019).
57. M. Becker, T. Guadalupe, B. Franke, D. P. Hibar, M. E. Renteria, J. L. Stein, P. M. Thompson, C. Francks, S. C. Vernes, S. E. Fisher, Early developmental gene enhancers affect subcortical volumes in the adult human brain. *Human brain mapping* **37**, 1788-1800 (2016).
58. L. Chen, A. E. Fish, J. A. Capra, Deep learning reveals evolutionary conservation and divergence of sequence properties underlying gene regulatory enhancers across mammals. *bioRxiv*, 110676 (2018).

59. A. R. Forrest, H. Kawaji, M. Rehli, J. K. Baillie, M. J. de Hoon, V. Haberle, T. Lassmann, I. V. Kulakovskiy, M. Lizio, M. Itoh, R. Andersson, C. J. Mungall, T. F. Meehan, S. Schmeier, N. Bertin, M. Jorgensen, E. Dimont, E. Arner, C. Schmidl, U. Schaefer, Y. A. Medvedeva, C. Plessy, M. Vitezic, J. Severin, C. Semple, Y. Ishizu, R. S. Young, M. Francescatto, I. Alam, D. Albanese, G. M. Altschuler, T. Arakawa, J. A. Archer, P. Arner, M. Babina, S. Rennie, P. J. Balwierz, A. G. Beckhouse, S. Pradhan-Bhatt, J. A. Blake, A. Blumenthal, B. Bodega, A. Bonetti, J. Briggs, F. Brombacher, A. M. Burroughs, A. Califano, C. V. Cannistraci, D. Carbajo, Y. Chen, M. Chierici, Y. Ciani, H. C. Clevers, E. Dalla, C. A. Davis, M. Detmar, A. D. Diehl, T. Dohi, F. Drablos, A. S. Edge, M. Edinger, K. Ekwall, M. Endoh, H. Enomoto, M. Fagiolini, L. Fairbairn, H. Fang, M. C. Farach-Carson, G. J. Faulkner, A. V. Favorov, M. E. Fisher, M. C. Frith, R. Fujita, S. Fukuda, C. Furlanello, M. Furino, J. Furusawa, T. B. Geijtenbeek, A. P. Gibson, T. Gingeras, D. Goldowitz, J. Gough, S. Guhl, R. Guler, S. Gustincich, T. J. Ha, M. Hamaguchi, M. Hara, M. Harbers, J. Harshbarger, A. Hasegawa, Y. Hasegawa, T. Hashimoto, M. Herlyn, K. J. Hitchens, S. J. Ho Sui, O. M. Hofmann, I. Hoof, F. Hori, L. Huminiecki, K. Iida, T. Ikawa, B. R. Jankovic, H. Jia, A. Joshi, G. Jurman, B. Kaczkowski, C. Kai, K. Kaida, A. Kaiho, K. Kajiyama, M. Kanamori-Katayama, A. S. Kasianov, T. Kasukawa, S. Katayama, S. Kato, S. Kawaguchi, H. Kawamoto, Y. I. Kawamura, T. Kawashima, J. S. Kempfle, T. J. Kenna, J. Kere, L. M. Khachigian, T. Kitamura, S. P. Klinken, A. J. Knox, M. Kojima, S. Kojima, N. Kondo, H. Koseki, S. Koyasu, S. Krampitz, A. Kubosaki, A. T. Kwon, J. F. Laros, W. Lee, A. Lennartsson, K. Li, B. Lilje, L. Lipovich, A. Mackay-Sim, R. Manabe, J. C. Mar, B. Marchand, A. Mathelier, N. Mejhert, A. Meynert, Y. Mizuno, D. A. de Lima Morais, H. Morikawa, M. Morimoto, K. Moro, E. Motakis, H. Motohashi, C. L. Mummery, M. Murata, S. Nagao-Sato, Y. Nakachi, F. Nakahara, T. Nakamura, Y. Nakamura, K. Nakazato, E. van Nimwegen, N. Ninomiya, H. Nishiyori, S. Noma, S. Noma, T. Noazaki, S. Ogishima, N. Ohkura, H. Ohimiya, H. Ohno, M. Ohshima, M. Okada-Hatakeyama, Y. Okazaki, V. Orlando, D. A. Ovchinnikov, A. Pain, R. Passier, M. Patrikakis, H. Persson, S. Piazza, J. G. Prendergast, O. J. Rackham, J. A. Ramilowski, M. Rashid, T. Ravasi, P. Rizzu, M. Roncador, S. Roy, M. B. Rye, E. Saijyo, A. Sajantila, A. Saka, S. Sakaguchi, M. Sakai, H. Sato, S. Savvi, A. Saxena, C. Schneider, E. A. Schultes, G. G. Schulze-Tanzil, A. Schwegmann, T. Sengstag, G. Sheng, H. Shimoji, Y. Shimoni, J. W. Shin, C. Simon, D. Sugiyama, T. Sugiyama, M. Suzuki, N. Suzuki, R. K. Swoboda, P. A. t Hoen, M. Tagami, N. Takahashi, J. Takai, H. Tanaka, H. Tatsukawa, Z. Tatum, M. Thompson, H. Toyodo, T. Toyoda, E. Valen, M. van de Wetering, L. M. van den Berg, R. Verado, D. Vijayan, I. E. Vorontsov, W. W. Wasserman, S. Watanabe, C. A. Wells, L. N. Winteringham, E. Wolvetang, E. J. Wood, Y. Yamaguchi, M. Yamamoto, M. Yoneda, Y. Yonekura, S. Yoshida, S. E. Zabierowski, P. G. Zhang, X. Zhao, S. Zucchelli, K. M. Summers, H. Suzuki, C. O. Daub, J. Kawai, P. Heutink, W. Hide, T. C. Freeman, B. Lenhard, V. B. Bajic, M. S. Taylor, V. J. Makeev, A. Sandelin, D. A. Hume, P. Carninci, Y. Hayashizaki, A promoter-level mammalian expression atlas. *Nature* **507**, 462-470 (2014).

60. C. C. Hon, J. A. Ramilowski, J. Harshbarger, N. Bertin, O. J. Rackham, J. Gough, E. Denisenko, S. Schmeier, T. M. Poulsen, J. Severin, M. Lizio, H. Kawaji, T. Kasukawa, M. Itoh, A. M. Burroughs, S. Noma, S. Djebali, T. Alam, Y. A. Medvedeva, A. C. Testa, L. Lipovich, C. W. Yip, I. Abugessaisa, M. Mendez, A. Hasegawa, D. Tang, T. Lassmann, P. Heutink, M. Babina, C. A. Wells, S. Kojima, Y. Nakamura, H. Suzuki, C. O. Daub, M. J. de Hoon, E. Arner, Y. Hayashizaki, P. Carninci, A. R. Forrest, An atlas of human long non-coding RNAs with accurate 5' ends. *Nature* **543**, 199-204 (2017).

61. X. Zheng, Y. Zheng, CscoreTool: fast Hi-C compartment analysis at high resolution. *Bioinformatics (Oxford, England)* **34**, 1568-1570 (2018).

62. M. Forcato, C. Nicoletti, K. Pal, C. M. Livi, F. Ferrari, S. Bicciato, Comparison of computational methods for Hi-C data analysis. *Nat Methods* **14**, 679-685 (2017).

63. R. Birnbaum, A. E. Jaffe, Q. Chen, T. M. Hyde, J. E. Kleinman, D. R. Weinberger, Investigation of the prenatal expression patterns of 108 schizophrenia-associated genetic loci. *Biological psychiatry* **77**, e43-51 (2015).

64. Human genomics. The Genotype-Tissue Expression (GTEx) pilot analysis: multitissue gene regulation in humans. *Science* **348**, 648-660 (2015).

65. *The NCBI Handbook [Internet]*. (National Center for Biotechnology Information, Bethesda, Maryland U.S.A., ed. 2nd Edition, 2013-).

66. I. Lee, U.M. Blom, P.I Wang, J.E. Shim, E.M. Marcotte, Prioritizing candidate disease genes by network-based boosting of genome-wide association data. *Genome research* **21**, 1109-1121 (2011).

67. M. J. Hawrylycz, E. S. Lein, A. L. Guillozet-Bongaarts, E. H. Shen, L. Ng, J. A. Miller, L. N. van de Lagemaat, K. A. Smith, A. Ebbert, Z. L. Riley, C. Abajian, C. F. Beckmann, A. Bernard, D. Bertagnolli, A. F. Boe, P. M. Cartagena, M. M. Chakravarty, M. Chapin, J. Chong, R. A. Dalley, B. David Daly, C. Dang,

S. Datta, N. Dee, T. A. Dolbeare, V. Faber, D. Feng, D. R. Fowler, J. Goldy, B. W. Gregor, Z. Haradon, D. R. Haynor, J. G. Hohmann, S. Horvath, R. E. Howard, A. Jeromin, J. M. Jochim, M. Kinnunen, C. Lau, E. T. Lazarz, C. Lee, T. A. Lemon, L. Li, Y. Li, J. A. Morris, C. C. Overly, P. D. Parker, S. E. Parry, M. Reding, J. J. Royall, J. Schulkin, P. A. Sequeira, C. R. Slaughterbeck, S. C. Smith, A. J. Sodt, S. M. Sunkin, B. E. Swanson, M. P. Vawter, D. Williams, P. Wohnoutka, H. R. Zielke, D. H. Geschwind, P. R. Hof, S. M. Smith, C. Koch, S. G. N. Grant, A. R. Jones, An anatomically comprehensive atlas of the adult human brain transcriptome. *Nature* **489**, 391-399 (2012).

68. M. Gartner, S. Aust, M. Bajbouj, Y. Fan, K. Wingenfeld, C. Otte, I. Heuser-Collier, H. Boker, J. Hattenschwiler, E. Seifritz, S. Grimm, M. Scheidegger, Functional connectivity between prefrontal cortex and subgenual cingulate predicts antidepressant effects of ketamine. *European neuropsychopharmacology : the journal of the European College of Neuropsychopharmacology* **29**, 501-508 (2019).
69. C. G. Abdallah, L. A. Averill, K. A. Collins, P. Geha, J. Schwartz, C. Averill, K. E. DeWilde, E. Wong, A. Anticevic, C. Y. Tang, D. V. Iosifescu, D. S. Charney, J. W. Murrough, Ketamine treatment and global brain connectivity in major depression. *Neuropsychopharmacology : official publication of the American College of Neuropsychopharmacology* **42**, 1210-1219 (2017).
70. J.A. Rinker, P.J. Mulholland, Promising pharmacogenetic targets for treating alcohol use disorder: evidence from preclinical models. *Pharmacogenomics* **18**, 555-570 (2017).
71. R.T. Timms, I.A. Tchasovnikarova, R. Antrobus, G. Dougan, P.J. Lehner, P. J. (2016). ATF7IP-mediated stabilization of the histone methyltransferase SETDB1 is essential for heterochromatin formation by the HUSH complex. *Cell reports* **17**, 653-659 (2016).
72. Z. Zhou, M. He, A.A Shah, Y. Wan, Insights into APC/C: from cellular function to diseases and therapeutics. *Cell division* **11**, 9 (2016).
73. E.A. Kramár, L.Y. Chen, N.J. Brandon, C.S. Rex, F. Liu, C.M. Gall, G. Lynch, Cytoskeletal changes underlie estrogen's acute effects on synaptic transmission and plasticity. *Journal of Neuroscience* **29**, 12982-12993 (2009).
74. P. Kerpedjiev, N. Abdennur, F. Lekschas, C. McCallum, K. Dinkla, H. Strobelt, J.M. Luber, S.B. Ouellette, A. Azhir, N. Kumar, J. Hwang, J., HiGlass: web-based visual exploration and analysis of genome interaction maps. *Genome biology* **19**, 125 (2018).
75. M. Haeussler, A. S. Zweig, C. Tyner, M. L. Speir, K. R. Rosenbloom, B. J. Raney, C. M. Lee, B. T. Lee, A. S. Hinrichs, J. N. Gonzalez, D. Gibson, M. Diekhans, H. Clawson, J. Casper, G. P. Barber, D. Haussler, R. M. Kuhn, W. J. Kent, The UCSC Genome Browser database: 2019 update. *Nucleic Acids Res* **47**, D853-d858 (2019).
76. G. Z. Reus, F. G. Vieira, H. M. Abelaira, M. Michels, D. B. Tomaz, M. A. dos Santos, A. S. Carlessi, M. V. Neotti, B. I. Matias, J. R. Luz, F. Dal-Pizzol, J. Quevedo, MAPK signaling correlates with the antidepressant effects of ketamine. *Journal of psychiatric research* **55**, 15-21 (2014).
77. Y. Shang, Y. Wu, S. Yao, X. Wang, D. Feng, W. Yang, Protective effect of erythropoietin against ketamine-induced apoptosis in cultured rat cortical neurons: involvement of PI3K/Akt and GSK-3 beta pathway. *Apoptosis : an international journal on programmed cell death* **12**, 2187-2195 (2007).
78. K. L. P. Garcia, A. D. Le, R. F. Tyndale, Brain CYP2B induction can decrease nicotine levels in the brain. *Addiction biology* **22**, 1257-1266 (2017).
79. Q. Liu, C. Chen, A. Gao, H.H. Tong, L. Xie, VariFunNet, an integrated multiscale modeling framework to study the effects of rare non-coding variants in genome-wide association studies: Applied to Alzheimer's disease. In *2017 IEEE International Conference on Bioinformatics and Biomedicine (BIBM)* (pp. 2177-2182). IEEE (2017).
80. L. Micheli, M. Ceccarelli, G. D'Andrea, F. Tirone, Depression and adult neurogenesis: Positive effects of the antidepressant fluoxetine and of physical exercise. *Brain research bulletin* **143**, 181-193 (2018).
81. S. J. Oh, J. Cheng, J. H. Jang, J. Arace, M. Jeong, C. H. Shin, J. Park, J. Jin, P. Greengard, Y. S. Oh, Hippocampal mossy cell involvement in behavioral and neurogenic responses to chronic antidepressant treatment. *Molecular psychiatry*, (2019).
82. P. Arnstein, M. Caudill, C. L. Mandle, A. Norris, R. Beasley, Self efficacy as a mediator of the relationship between pain intensity, disability and depression in chronic pain patients. *Pain* **80**, 483-491 (1999).
83. M. A. Peltoniemi, N. M. Hagelberg, K. T. Olkkola, T. I. Saari, Ketamine: A review of clinical pharmacokinetics and pharmacodynamics in anesthesia and pain therapy. *Clinical pharmacokinetics* **55**, 1059-1077 (2016).
84. Gerard Sanacora, M.D. , and, Rachel Katz, M.D., Ketamine: A review for clinicians. *FOCUS* **16**, 243-250 (2018).

85. J. de Leon, F. J. Diaz, A meta-analysis of worldwide studies demonstrates an association between schizophrenia and tobacco smoking behaviors. *Schizophrenia research* **76**, 135-157 (2005).
86. A. Hunter, R. Murray, L. Asher, J. Leonardi-Bee, The effects of tobacco smoking, and prenatal tobacco smoke exposure, on risk of schizophrenia: a systematic review and meta-analysis. *Nicotine & tobacco research : official journal of the Society for Research on Nicotine and Tobacco*, (2018).
87. J. G. Scott, L. Matuschka, S. Niemela, J. Miettunen, B. Emmerson, A. Mustonen, Evidence of a Causal Relationship Between Smoking Tobacco and Schizophrenia Spectrum Disorders. *Frontiers in psychiatry* **9**, 607 (2018).
88. Y. Zhou, M. Ingelman-Sundberg, V. M. Lauschke, Worldwide Distribution of Cytochrome P450 Alleles: A Meta-analysis of Population-scale Sequencing Projects. *Clinical pharmacology and therapeutics* **102**, 688-700 (2017).
89. A. J. Bloom, M. Martinez, L. S. Chen, L. J. Bierut, S. E. Murphy, A. Goate, CYP2B6 non-coding variation associated with smoking cessation is also associated with differences in allelic expression, splicing, and nicotine metabolism independent of common amino-acid changes. *PloS one* **8**, e79700 (2013).
90. Y. Li, J. K. Coller, M. R. Hutchinson, K. Klein, U. M. Zanger, N. J. Stanley, A. D. Abell, A. A. Somogyi, The CYP2B6*6 allele significantly alters the N-demethylation of ketamine enantiomers in vitro. *Drug metabolism and disposition: the biological fate of chemicals* **41**, 1264-1272 (2013).
91. Y. Li, K. A. Jackson, B. Slon, J. R. Hardy, M. Franco, L. William, P. Poon, J. K. Coller, M. R. Hutchinson, D. C. Currow, A. A. Somogyi, CYP2B6*6 allele and age substantially reduce steady-state ketamine clearance in chronic pain patients: impact on adverse effects. *British journal of clinical pharmacology* **80**, 276-284 (2015).
92. D. P. Herzog, G. Wegener, K. Lieb, M. B. Muller, G. Treccani, Decoding the mechanism of action of rapid-acting antidepressant treatment strategies: Does gender matter? *International journal of molecular sciences* **20**, (2019).
93. D.S. Wishart, Y.D. Feunang, A.C. Guo, E.J. Lo, A. Marcu, J.R. Grant, T. Sajed, D. Johnson, C. Li, Z. Sayeeda, N. Assempour, N., DrugBank 5.0: a major update to the DrugBank database for 2018. *Nucleic acids research*, **46**, D1074-D1082 (2017).
94. O. Ursu, J. Holmes, C.G. Bologa, J.J. Yang, S.L. Mathias, V. Stathias, D.T. Nguyen, S. Schürer, T. Oprea, DrugCentral 2018: an update. *Nucleic acids research*, **47**, D963-D970 (2018).
95. D.Y.L. Barbará, J. Couto, COOLCAT: an entropy-based algorithm for categorical clustering. In *Proceedings of the eleventh international conference on Information and knowledge management*, pp. 582-589. ACM (2002).
96. D. Thissen, L. Steinberg, D. Kuang, Quick and easy implementation of the Benjamini-Hochberg procedure for controlling the false positive rate in multiple comparisons. *Journal of educational and behavioral statistics* **27**, 77-83 (2002).

SUPPLEMENT

Ketamine Pharmacogenomic Network in Human Brain Contains Sub-Networks Associated with Glutamate Neurotransmission and with Neuroplasticity

Authors: Gerald A. Higgins[1, 2], Samuel A. Handelman[3], Ari Allyn-Feuer[1]†, Alex S. Ade[1, 2], James S. Burns[2], Gilbert S. Omenn[1, 3, 4, 5], Brian D. Athey[1, 2, 6]*

Affiliations:

[1]Department of Computational Medicine and Bioinformatics, University of Michigan Medical School, Ann Arbor, MI 48109, USA.

[2]Phenomics Health Inc., Ann Arbor, MI 48109, USA.

[3]Department of Internal Medicine, University of Michigan Medical School, Ann Arbor, MI 48109, USA.

[4]School of Public Health, University of Michigan, Ann Arbor, MI 48109, USA.

[5]Department of Human Genetics, University of Michigan Medical School, Ann Arbor, MI 48109, USA.

[6]Department of Psychiatry, University of Michigan Medical School, Ann Arbor, MI 48109, USA.

*Corresponding author: Email: bleu@med.umich.edu (B.D.A.)

†Current address: GlaxoSmithKline, King of Prussia, PA 19406, USA.

Table of Contents

Supplementary Table 1: Functional neuroimaging studies used to build consensus map:

TITLE	PARTICIPANTS	KETAMINE'S SITE(S) OF ACTION	MOD.	PMID
Effects of sub-anesthetic doses of ketamine on regional cerebral blood flow, oxygen consumption, and blood volume in humans	9 healthy controls	Anterior cingulate cortex (ACC) and prefrontal cortex (PFC). Not recognized – anterior caudate (AC) and nucleus accumbens (NA).	PET	12960545
Effects of ketamine on anterior cingulate glutamate metabolism in healthy humans: a 4-T proton MRS study	10 healthy controls	Anterior cingulate cortex (ACC).	1H-MRS	15677610
Increased anterior cingulate cortical activity in response to fearful faces: A neurophysiological biomarker that predicts rapid antidepressant response to ketamine	11 healthy controls and 11 drug-free patients diagnosed with MDD	Patients with MDD exhibited increased activity in the anterior cingulate cortex (ACC) after pretreatment with fearful faces versus controls. Also, changes observed in right amygdala (AMY).	MEG	18822408
Anterior cingulate desynchronization and functional connectivity with the amygdala during a working memory task predict rapid antidepressant response to ketamine	15 drug-free patients diagnosed with MDD	Subgenual anterior cingulate cortex (ACC), supplementary motor area (SMA) and amygdala (AMY).	MEG	20393460
Ketamine decreases resting state functional network connectivity in healthy subjects: Implications for antidepressant drug action	17 healthy controls	Subgenual anterior cingulate cortex (sgACC), dorsomedial prefrontal cortex (PFC),	fMRI BOLD	23049758
Relationship of resting brain hyperconnectivity and schizophrenia-like symptoms produced by the NMDA receptor antagonist ketamine in humans	22 healthy controls; Replication in another 12 healthy controls	Ketamine administration increased global brain connectivity. Psychotomimetic (negative) effects following ketamine administration were localized to the nucleus accumbens (NA) and anterior caudate (AC). Positive symptoms were associated with changes in prefrontal cortex (PFC), supplementary motor area (SM), insula and posterior cortex.	rs-fcMRI	23337947
Neural correlates of rapid antidepressant response to ketamine in treatment-resistant unipolar depression: A preliminary PET study	20 drug-free patients diagnosed with TRD	Anterior cingulate cortex (ACC), prefrontal cortex (PFC), amygdala (AMY) and habenula.	PET	23540908
Neural correlates of rapid antidepressant response to ketamine in bipolar disorder	21 patients with bipolar depression	Sub-geniculate anterior cingulate cortex (ACC), supplementary motor area (SMA), prefrontal cortex (PFC). Also, unrecognized, but included amygdala (AMY), hippocampal formation (HF), anterior caudate (AC) and nucleus accumbens (NA).	PET	24103187

Anti-anhedonic effect of ketamine and its neural correlates in treatment-resistant bipolar depression	36 patients who are treatment-refractory diagnosed with bipolar disorder I or II	Ketamine significantly activated the dorsal anterior cingulate cortex (dACC) and the subcortex.	PET	25313512
Neural correlates of change in major depressive disorder anhedonia following open-label ketamine.	52 patients diagnosed with TRD	Supplementary motor area (SMA), hippocampal formation (HF), frontal gyrus and orbitofrontal cortex correlated with measures of decreased anhedonia in patients diagnosed with MDD. *Borderline significance.*	PET	25691504
A pilot in vivo proton magnetic resonance spectroscopy study of amino acid neurotransmitter response to ketamine treatment of major depressive disorder	11 patients diagnosed with MDD	Prefrontal cortex (PFC).	1H-MRS	26283639
The effects of low-dose ketamine on the prefrontal cortex and amygdala in treatment-resistant depression: A randomized controlled study	48 patients diagnosed with TRD	Prefrontal cortex (PFC), amygdala (AMY) and supplementary motor area (SMA).	PET	26821769
Ketamine modulates subgenual cingulate connectivity with the memory-related neural circuit-a mechanism of relevance to resistant depression?	13 healthy controls	Following ketamine infusion, largest changes observed in the connectivity of the subgenual anterior cingulate cortex (sgACC).	fMRI	26925332
Comparing the actions of Lanicemine and ketamine in depression : key role of the anterior cingulate	60 un-medicated patients diagnosed with MDD	Intravenous infusion of both ketamine and Lanicemine gradually increased activity in the subgenual anterior cingulate cortex (sgACC).	phMRI	27133029
Ketamine modulates hippocampal neurochemistry and functional connectivity – A combined magnetic resonance spectroscopy and resting state fMRI study in healthy volunteers	15 healthy controls	Dorsomedial prefrontal cortex (PFC) and anterior cingulate cortex (ACC). Psychosis severity produced by ketamine was associated with increased connectivity of the hippocampal formation (HF) with the middle cingulate cortex, insula, precuneus and superior frontal gyrus.	rs-fcMRI; 1H-MRS	27480949
Ketamine treatment and global brain connectivity in major depression	25 healthy controls and 18 drug-free patients diagnosed with MDD	Subgenual anterior cingulate cortex (sgACC), dorsolateral prefrontal cortex and dorsomedial prefrontal cortex (PFC), anterior caudate (AC), nucleus accumbens (NA).	rs-fcMRI	27604566

The nucleus accumbens and ketamine treatment in major depressive disorder	The first cohort was 34 patients diagnosed with MDD and 26 healthy controls. The second cohort was 16 patients diagnosed with MDD.	The volume of the nucleus accumbens (NA) was altered in MDD patients, while hippocampal formation (HF) volume was increased following ketamine in MDD patients who exhibited remission.	1H-MRS	28272497
Persistent antidepressant effect of low dose ketamine and activation in the supplementary motor area and anterior cingulate cortex in tre atment-resistant depression: A randomized control study	24 patients diagnosed with TRD	TRD patients receiving the 0.5mg/kg ketamine infusion exhibited activation in supplementary motor area (SMA) and anterior cingulate cortex (ACC) than did those receiving the 0.2mg/kg ketamine infusion. The increase in the SUV in the ACC was negatively correlated with depressive symptoms after ketamine infusion.	PET	28922734
Glutamate levels and resting cerebral blood flow in anterior cingulate cortex are associated at rest and immediately following infusion of S-ketamine in healthy volunteers	25 healthy controls	Dorsomedial prefrontal cortex (PFC) and anterior cingulate cortex (ACC).	1H-MRS	29467681
Default mode connectivity in major depressive disorder measured up to 10 days after ketamine administration	33 patients diagnosed with MDD and 25 healthy controls in a cross-over study	MDD patients exhibited normalization of connectivity between the insular cortex (IC), posterior anterior cingulate cortex (pACC) and subgenual anterior cingulate cortex (sgACC).	fMRI	29580569
7T 1 H-MRS in major depressive disorder: A Ketamine Treatment Study	17 healthy controls and 20 patients diagnosed with MDD	Different MDD phenotypes exhibited different brain region alterations following ketamine infusions, ranging from sub-geniculate anterior cingulate cortex (ACC) to anterior caudate (AC).	1H-MRS	29748628
Pharmacological fMRI: Effects of sub-anesthetic ketamine on resting-state functional connectivity in the default mode network, salience network, dorsal attention network and executive control network	17 healthy male subjects	Anterior cingulate cortex (ACC), superior frontal gyrus including supplementary motor area (SMA), amygdala (AMY), hippocampal formation (HF), anterior caudate (AC), nucleus accumbens (NA), prefrontal cortex (PFC).	rs-fcMRI	30003027
Ketamine, but Not the NMDAR antagonist Lanicemine, Increases prefrontal global connectivity in depressed patients	56 un-medicated patients diagnosed with MDD	Ketamine increased global connectivity of the prefrontal cortex (PFC) in depressed patients.	fMRI	30263977

Functional connectivity between prefrontal cortex and Subgenual cingulate predicts antidepressant effects of ketamine	24 patients diagnosed with MDD	A single sub-anesthetic dose of ketamine increased functional connectivity between prefrontal Cortex (PFC) and the subgenual anterior cingulate cortex (sgACC).	rs-fcMRI	30819549
NEGATIVE RESULTS				
TITLE	**PARTICIPANTS**	**KETAMINE'S SITE(S) OF ACTION**	**MOD.**	**PMID**
The antidepressant effect of ketamine is not associated with changes in occipital amino acid neurotransmitter content as measured by [^{1}H]-MRS	10 patients diagnosed with MDD	Rapid (1 hour) and sustained (7 days) antidepressant effects produced by ketamine were not associated with changes in amino acid neurotransmitter content in occipital cortex (OC).	1H-MRS	21232924

Neuroimaging modalities (MOD.):
1H-MRS: 4-T 1H proton magnetic resonance spectroscopy
fMRI: Functional magnetic resonance imaging.
MEG: Magnetoencephalography;
PET: FDG positron emission tomography;
phMRI; Pharmacological magnetic resonance imaging.
rs-fcMRI: resting-state functional connectivity magnetic resonance imaging.

Supplementary Table 2A. Gene symbols, ketamine glutamate receptor sub-network

Gene symbol	Gene name (HGNC)	Location	Protein product
ACHE	acetylcholinesterase (Cartwright blood group)	Plasma Membrane	enzyme
ATF7IP	activating transcription factor 7 interacting protein	Nucleus	transcription regulator
ATF7IP2	activating transcription factor 7 interacting protein 2	Nucleus	other
ATP1A1	ATPase Na+/K+ transporting subunit alpha 1	Plasma Membrane	transporter
BORCS7	BLOC-1 related complex subunit 7	Cytoplasm	other
BRD4	bromodomain containing 4	Nucleus	kinase
CACNA1C	calcium voltage-gated channel subunit alpha1 C	Plasma Membrane	ion channel
CACNB1	calcium voltage-gated channel auxiliary subunit beta 1	Plasma Membrane	ion channel
CACNB2	calcium voltage-gated channel auxiliary subunit beta 2	Plasma Membrane	ion channel
CACNG2	calcium voltage-gated channel auxiliary subunit gamma 2	Plasma Membrane	ion channel
CHRM2	cholinergic receptor muscarinic 2	Plasma Membrane	G-protein coupled receptor
CHRNA3	cholinergic receptor nicotinic alpha 3 subunit	Plasma Membrane	transmembrane receptor
CHRNA5	cholinergic receptor nicotinic alpha 5 subunit	Plasma Membrane	transmembrane receptor
CHRNA7	cholinergic receptor nicotinic alpha 7 subunit	Plasma Membrane	transmembrane receptor
CNR1	cannabinoid receptor 1	Plasma Membrane	G-protein coupled receptor
DLG3	discs large MAGUK scaffold protein 3	Plasma Membrane	kinase
DLG4	discs large MAGUK scaffold protein 4	Plasma Membrane	kinase
DNMT1	DNA methyltransferase 1	Nucleus	enzyme
EHMT1	euchromatic histone lysine methyltransferase 1	Nucleus	transcription regulator
GABRA2	gamma-aminobutyric acid type A receptor alpha2 subunit	Plasma Membrane	ion channel
GABRA5	gamma-aminobutyric acid type A receptor alpha5 subunit	Plasma Membrane	ion channel
GAD1	glutamate decarboxylase 1	Cytoplasm	enzyme
GLRA1	glycine receptor alpha 1	Plasma Membrane	ion channel
GLRA2	glycine receptor alpha 2	Plasma Membrane	ion channel
GLRB	glycine receptor beta	Plasma Membrane	ion channel
GRIA1	glutamate ionotropic receptor AMPA type subunit 1	Plasma Membrane	ion channel
GRIA2	glutamate ionotropic receptor AMPA type subunit 2	Plasma Membrane	ion channel
GRIA4	glutamate ionotropic receptor AMPA type subunit 4	Plasma Membrane	ion channel
GRIN1	glutamate ionotropic receptor NMDA type subunit 1	Plasma Membrane	ion channel
GRIN2A	glutamate ionotropic receptor NMDA type subunit 2A	Plasma Membrane	ion channel
GRIN2B	glutamate ionotropic receptor NMDA type subunit 2B	Plasma Membrane	ion channel
GRIN2C	glutamate ionotropic receptor NMDA type subunit 2C	Plasma Membrane	ion channel
GRIN2D	glutamate ionotropic receptor NMDA type subunit 2D	Plasma Membrane	ion channel
GRIN3A	glutamate ionotropic receptor NMDA type subunit 3A	Plasma Membrane	ion channel
GRIN3B	glutamate ionotropic receptor NMDA type subunit 3B	Plasma Membrane	ion channel
HCN1	hyperpolarization activated cyclic nucleotide gated potassium channel 1	Plasma Membrane	ion channel
HDAC5	histone deacetylase 5	Nucleus	transcription regulator
MBD1	methyl-CpG binding domain protein 1	Nucleus	transcription regulator
MPHOSPH8	M-phase phosphoprotein 8	Nucleus	transcription regulator
NCAM1	neural cell adhesion molecule 1	Plasma Membrane	other
NOS1	nitric oxide synthase 1	Cytoplasm	enzyme
NOS2	nitric oxide synthase 2	Cytoplasm	enzyme
NOS3	nitric oxide synthase 3	Cytoplasm	enzyme
NQO1	NAD(P)H quinone dehydrogenase 1	Cytoplasm	enzyme
OPRK1	opioid receptor kappa 1	Plasma Membrane	G-protein coupled receptor
OPRM1	opioid receptor mu 1	Plasma Membrane	G-protein coupled receptor
ROBO2	roundabout guidance receptor 2	Plasma Membrane	transmembrane receptor
SETDB1	SET domain bifurcated histone lysine methyltransferase 1	Nucleus	enzyme
SHANK2	SH3 and multiple ankyrin repeat domains 2	Plasma Membrane	other
SIGMAR1	sigma non-opioid intracellular receptor 1	Plasma Membrane	transmembrane receptor
SLC6A9	solute carrier family 6 member 9	Plasma Membrane	transporter
TASOR	transcription activation suppressor	Nucleus	other
TOGARAM2	TOG array regulator of axonemal microtubules 2	Other	other
TRIM28	tripartite motif containing 28	Nucleus	transcription regulator
ZNF274	zinc finger protein 274	Nucleus	transcription regulator

Supplementary Table 2B. Gene symbols, ketamine neuroplasticity sub-network

Gene symbol	Gene name (HGNC)	Location	Protein product
ARC	activity regulated cytoskeleton associated protein	Cytoplasm	other
ASCL1	achaete-scute family bHLH transcription factor 1	Nucleus	transcription regulator
BDNF	brain derived neurotrophic factor	Extracellular Space	growth factor
BDNF-AS	BDNF antisense RNA	Other	other
CAMK2A	calcium/calmodulin dependent protein kinase II alpha	Cytoplasm	kinase
CDKN1A	cyclin dependent kinase inhibitor 1A	Nucleus	kinase
CREM	cAMP responsive element modulator	Nucleus	transcription regulator
CUX2	cut like homeobox 2	Nucleus	transcription regulator
DCC	DCC netrin 1 receptor	Plasma Membrane	transmembrane receptor
DRD2	dopamine receptor D2	Plasma Membrane	G-protein coupled receptor
EEF2K	eukaryotic elongation factor 2 kinase	Cytoplasm	kinase
FMR1	fragile X mental retardation 1	Cytoplasm	translation regulator
GDAP1L1	ganglioside induced differentiation associated protein 1 like 1	Other	other
GRM5	glutamate metabotropic receptor 5	Plasma Membrane	G-protein coupled receptor
HOMER1	homer scaffold protein 1	Plasma Membrane	other
HTR1B	5-hydroxytryptamine receptor 1B	Plasma Membrane	G-protein coupled receptor
HTR2A	5-hydroxytryptamine receptor 2A	Plasma Membrane	G-protein coupled receptor
KLF6	Kruppel like factor 6	Nucleus	transcription regulator
LIN7C	lin-7 homolog C, crumbs cell polarity complex component	Cytoplasm	other
ENSG00000251574		Nucleus	RNA gene
MEF2D	myocyte enhancer factor 2D	Nucleus	transcription regulator
MYO6	myosin VI	Cytoplasm	other
MYT1L	myelin transcription factor 1 like	Nucleus	transcription regulator
NEUROD1	neuronal differentiation 1	Nucleus	transcription regulator
NEUROD2	neuronal differentiation 2	Nucleus	transcription regulator
NHLH2	nescient helix-loop-helix 2	Nucleus	transcription regulator
NMB	neuromedin B	Extracellular Space	other
NSMF	NMDA receptor synaptonuclear signaling and neuronal migration factor	Extracellular Space	other
NTRK2	neurotrophic receptor tyrosine kinase 2	Plasma Membrane	kinase
PTEN	phosphatase and tensin homolog	Cytoplasm	phosphatase
PTGS2	prostaglandin-endoperoxide synthase 2	Cytoplasm	enzyme
RAC1	Rac family small GTPase 1	Plasma Membrane	enzyme
RASGRF2	Ras protein specific guanine nucleotide releasing factor 2	Cytoplasm	other
RHOA	ras homolog family member A	Cytoplasm	enzyme
ROBO2	roundabout guidance receptor 2	Plasma Membrane	transmembrane receptor
ENSG00000225960		Nucleus	RNA gene
SEMA3A	semaphorin 3A	Extracellular Space	other
SHANK1	SH3 and multiple ankyrin repeat domains 1	Cytoplasm	other
SHANK2	SH3 and multiple ankyrin repeat domains 2	Plasma Membrane	other
SHANK3	SH3 and multiple ankyrin repeat domains 3	Plasma Membrane	other
SLC22A15	solute carrier family 22 member 15	Other	transporter
SLC6A2	solute carrier family 6 member 2	Plasma Membrane	transporter
SLIT1	slit guidance ligand 1	Extracellular Space	other
SLIT2	slit guidance ligand 2	Extracellular Space	other
SNAP25	synaptosome associated protein 25	Plasma Membrane	transporter
SYN1	synapsin I	Plasma Membrane	transporter
SYN2	synapsin II	Plasma Membrane	other
SYT3	synaptotagmin 3	Cytoplasm	transporter
TBR1	T-box, brain 1	Nucleus	transcription regulator
TCF4	transcription factor 4	Nucleus	transcription regulator

Supplementary Table 2C. Gene symbols, ketamine pharmacokinetic receptor sub-network

Gene symbol	Gene name (HGNC)	Location	Protein product
ANAPC2	anaphase promoting complex subunit 2	Nucleus	other
CYP2A6	cytochrome P450 family 2 subfamily A member 6	Cytoplasm	enzyme
CYP2B6	cytochrome P450 family 2 subfamily B member 6	Cytoplasm	enzyme
CYP3A4	cytochrome P450 family 3 subfamily A member 4	Cytoplasm	enzyme
ESR1	estrogen receptor 1	Nucleus	ligand-dependent nuclear receptor
TCERG1	transcription elongation regulator 1	Nucleus	transcription regulator

TARGET	SPECIES	BINDING AFFINITY / INHIBITION CONSTANT	STEREOSELECTIVITY	PMID
AMPAR: GRIA1, GRIA2, GRIA4	Human	K_i = 7 ± 0.5 μM (SK), 24.5 ± 2.0 μM (RK)	SK has 3.5-fold affinity of RK	29945898
NMDAR: GRIN1, GRIN2A, GRIN2B, GRIN2C, GRIN2D, GRIN3A, GRIN3B	Human	K_i = 0.7 ± 0.3 μM (SK), 2.3 ± 0.3 μM (RK)	SK has 3-fold affinity of RK	29945898
NMDAR: GRIN1, GRIN2A, GRIN2B, GRIN2C, GRIN2D, GRIN3A, GRIN3B	Human	K_i = 0.06 ± 0.1 μM	Not measured	1311263
CACNA1C	Rat	IC_{50} = 9.2 μM	Not measured	29945898
CHRM2	Human	K_i = 7.4 ± 4.5 μM	No observed difference	29945898
CNR1	Human	K_i = 42 ± 5 μM	Not measured	24093505
CHRNA3	Human	IC_{50} = 50μM	Not measured	29945898
CHRNA5	Human	IC_{50} = 5μM	Not measured	29945898
CHRNA7	Human	K_i = 12 ± 0.8 μM	No observed difference	29945898
DRD2	Human	K_i = 12 ± 0.8 μM	Not measured	12232776
DRD2	Rat	K_i = 1 ± 0.2 μM	Not measured	30034974
ESR1	Human	K_i = 94 ± 8 μM	No observed difference	29945898
GABRA1	Human	K_i = 134 ± 29 μM	Not measured	29945898
GABBR1	Human	K_i = 144 ± 32 μM	Not measured	29945898
GABRA2	Guinea pig	K_i = 1 ± 0.7 μM (RK), 12.2 ± 1.2 μM (SK)	RK has 12-fold affinity of SK	29945898
GABRA5	Rat	K_i = 10 ± 1.1 μM	No observed difference	29945898
GLRB	Human	K_i = 27 ± 7.2 μM	Not measured	29945898
GRM5	Rat	K_i = 7 ± 0.62 μM	Not measured	30034974
HCN1	Rat PC12 cells	K_i = 0.035 ± 0.3 μM (RK), 54 ± 3.7 μM (SK)	RK has 5000-fold affinity of SK	29945898
HCN1	Human	EC_{50} = 4.1 μM – 7.1 μM (SK)	Not measured	29945898
HTR3A	Human	IC_{50} = 910 ± 30 μM	Not measured	10754635
HTR2A	Human	K_i = 19 μM (RK), 135 μM (SK),	RK has 7-fold affinity of SK	29945898
HTR1A	Human	IC_{50} = 46 ± 1.4 μM	Not measured	29945898
HTR1B	Human	K_i = 6 ± 0.2 μM	Not measured	29945898
OPRM1	Guinea pig	K_i = 11 μM (SK), 28□μM (RK)	SK has 2.5-fold affinity of RK	8835358
OPRD1	Guinea pig	K_i = 130 μM (SK), 130□ μM (RK)	No significant difference	8835358
OPRK1	CHO	K_i = 4.2 ± 0.03 μM (SK), 4.6 ± 0.04 μM (RK)	No significant difference	9915326
SIGMAR1	Rat brain	K_i = 19 μM (RK), 200 μM (SK)	RK has 10-fold affinity of SK	29945898
SLC6A2	Human	K_i = 67 ± 26 μM	Not measured	9523822
SLC6A3	Human	K_i = 46.9 μM (SK), 390 μM (RK)	SK has 8-fold affinity of RK	10553955
SLC6A4	Rat	K_i = 162 ± 28 μM	Not measured	9523822

Supplementary Table 3. Ketamine binding affinity studies. Affinity of ketamine to various CNS targets as measured by displacement of radiolabeled ligands or radioligand assays. **Molecules in bold text were added to the ketamine network based on the high affinity binding of ketamine.** CHO: Chinese hamster ovary cells; PubMed ID numbers refers to where the original studies can be found at the PubMed web site, National Library of Medicine **(65).**

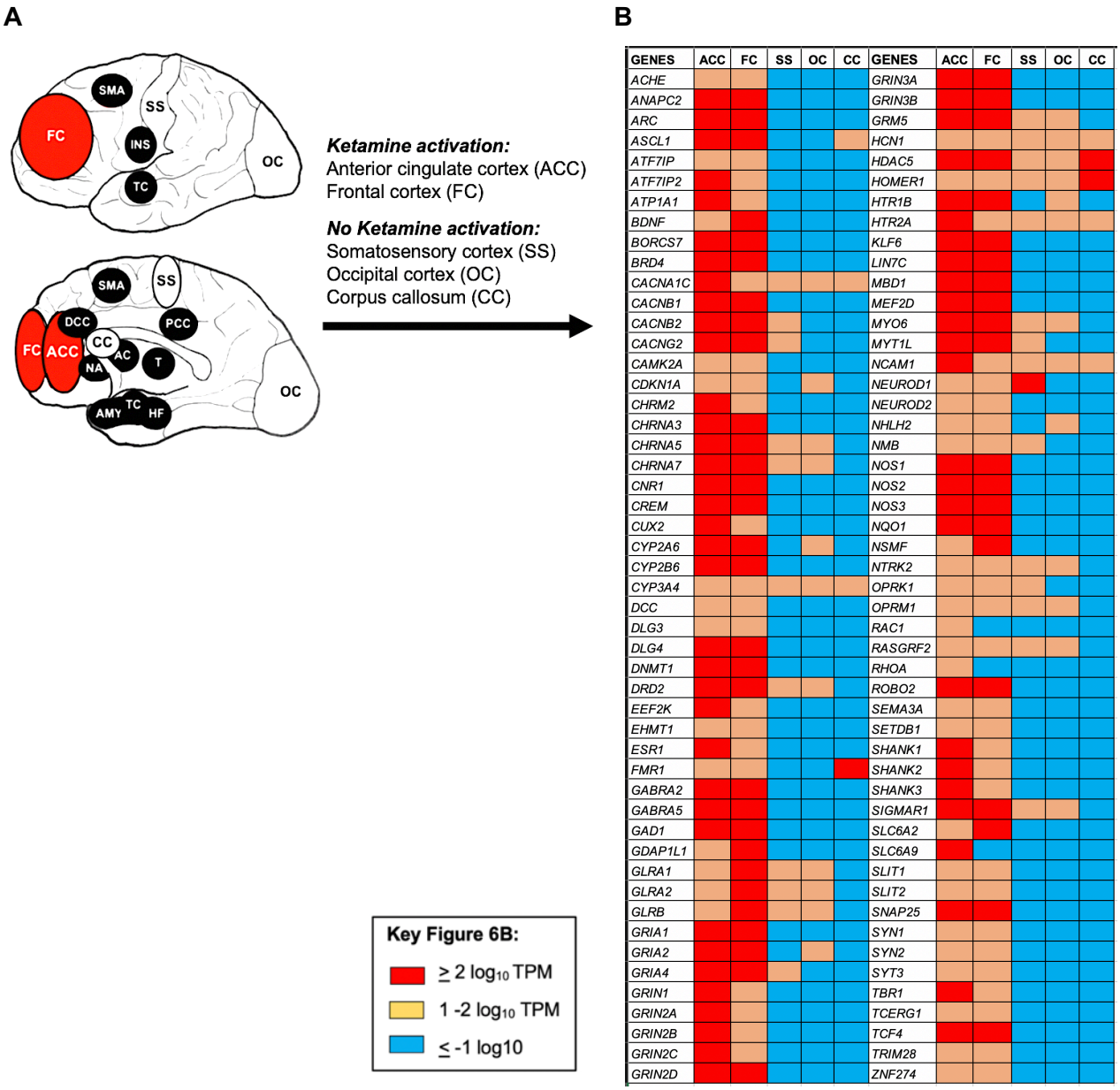

GENES	ACC	FC	SS	OC	CC	GENES	ACC	FC	SS	OC	CC
ACHE						*GRIN3A*					
ANAPC2						*GRIN3B*					
ARC						*GRM5*					
ASCL1						*HCN1*					
ATF7IP						*HDAC5*					
ATF7IP2						*HOMER1*					
ATP1A1						*HTR1B*					
BDNF						*HTR2A*					
BORCS7						*KLF6*					
BRD4						*LIN7C*					
CACNA1C						*MBD1*					
CACNB1						*MEF2D*					
CACNB2						*MYO6*					
CACNG2						*MYT1L*					
CAMK2A						*NCAM1*					
CDKN1A						*NEUROD1*					
CHRM2						*NEUROD2*					
CHRNA3						*NHLH2*					
CHRNA5						*NMB*					
CHRNA7						*NOS1*					
CNR1						*NOS2*					
CREM						*NOS3*					
CUX2						*NQO1*					
CYP2A6						*NSMF*					
CYP2B6						*NTRK2*					
CYP3A4						*OPRK1*					
DCC						*OPRM1*					
DLG3						*RAC1*					
DLG4						*RASGRF2*					
DNMT1						*RHOA*					
DRD2						*ROBO2*					
EEF2K						*SEMA3A*					
EHMT1						*SETDB1*					
ESR1						*SHANK1*					
FMR1						*SHANK2*					
GABRA2						*SHANK3*					
GABRA5						*SIGMAR1*					
GAD1						*SLC6A2*					
GDAP1L1						*SLC6A9*					
GLRA1						*SLIT1*					
GLRA2						*SLIT2*					
GLRB						*SNAP25*					
GRIA1						*SYN1*					
GRIA2						*SYN2*					
GRIA4						*SYT3*					
GRIN1						*TBR1*					
GRIN2A						*TCERG1*					
GRIN2B						*TCF4*					
GRIN2C						*TRIM28*					
GRIN2D						*ZNF274*					

Supplementary Fig. 1. Consensus between ketamine pharmacogenomic pathway gene expression in human brain and regions where ketamine exerts a rapid antidepressant effect derived from functional imaging studies (Supplementary Table 1). (A) Human brain regions impacted by ketamine projected onto lateral (top) and medial (bottom) surfaces of the brain. Black indicates ketamine activation regions and dark red indicates those CNS areas first activated by the drug. **(B)** Expression of 100 out of 107 genes in the ketamine pharmacogenomic pathway whose expression could be determined. Abbreviations: **ACC**: Anterior cingulate cortex; **AC**: Anterior caudate; **AMY**: Amygdala; **CC**: Corpus callosum; **dACC**: Dorsal anterior cingulate cortex; **FC**: Frontal cortex; **HF**: Hippocampal formation; **INS**: Insular cortex; **NA**: Nucleus accumbens; **OC**: Occipital cortex; **pCC**: Posterior cingulate cortex; **PFC**: Prefrontal cortex; **SMA**: Supplementary motor area; **Supplementary Figure 3.** Examples of *in situ* hybridization of selected super-pathway genes that are ketamine PD targets, from the human brain atlas of the Allen Brain Science Institute **(62) sgACC**: Subgenual anterior cingulate cortex; **SS**: Somatosensory cortex; **T**: Thalamus; **TC**: Temporal cortex; **TPM**: Transcripts per million.

Supplementary Figure 2. Examples of *in situ* hybridization of selected super-pathway genes that are ketamine PD targets, from **(62)**

Amygdala

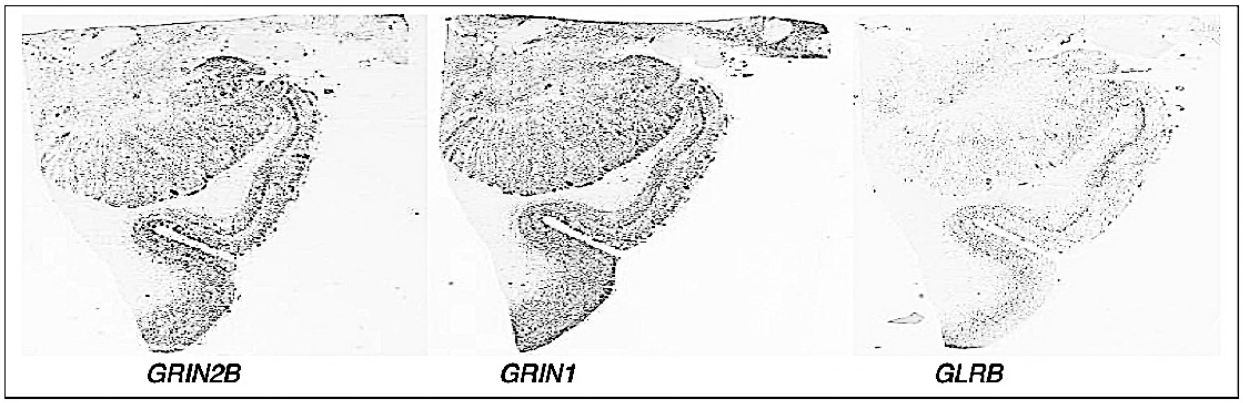

Hippocampal formation

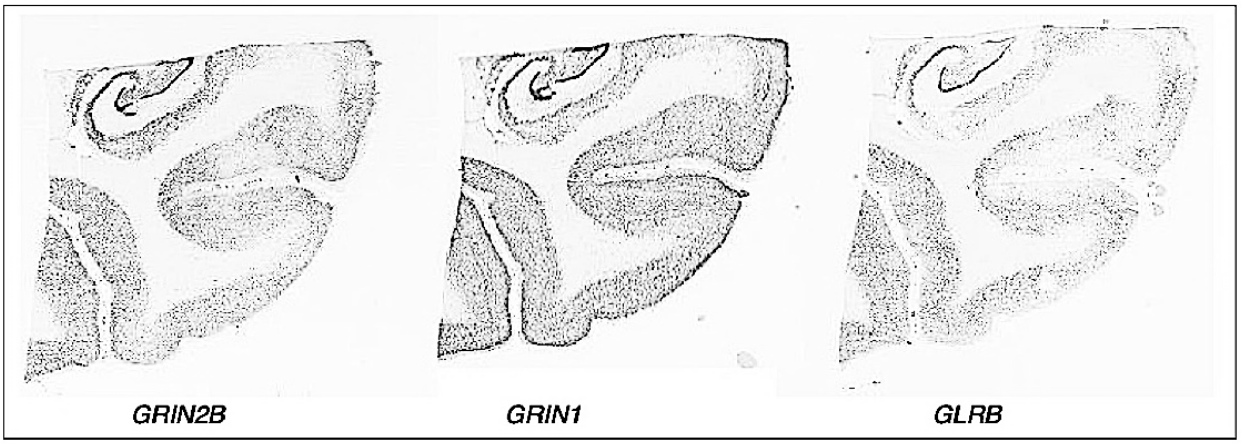

Anterior caudate (AC), nucleus accumbens (NA), putamen (P) and globus pallidus

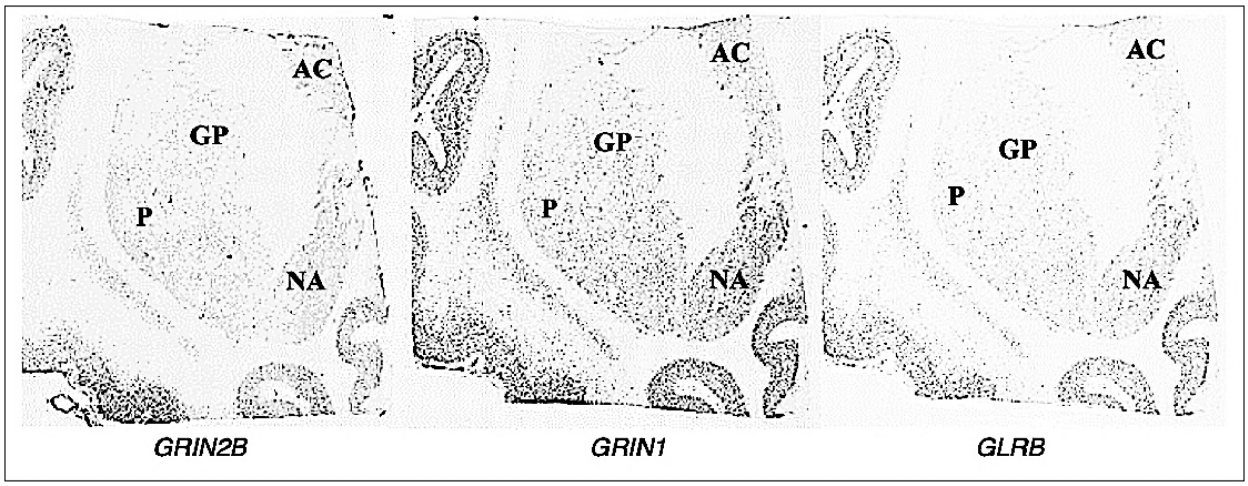

Supplementary Figure 2. Examples of *in situ* hybridization of selected super-pathway genes that are ketamine PD targets, from **(62)**, *continued*

Anterior cingulate cortex

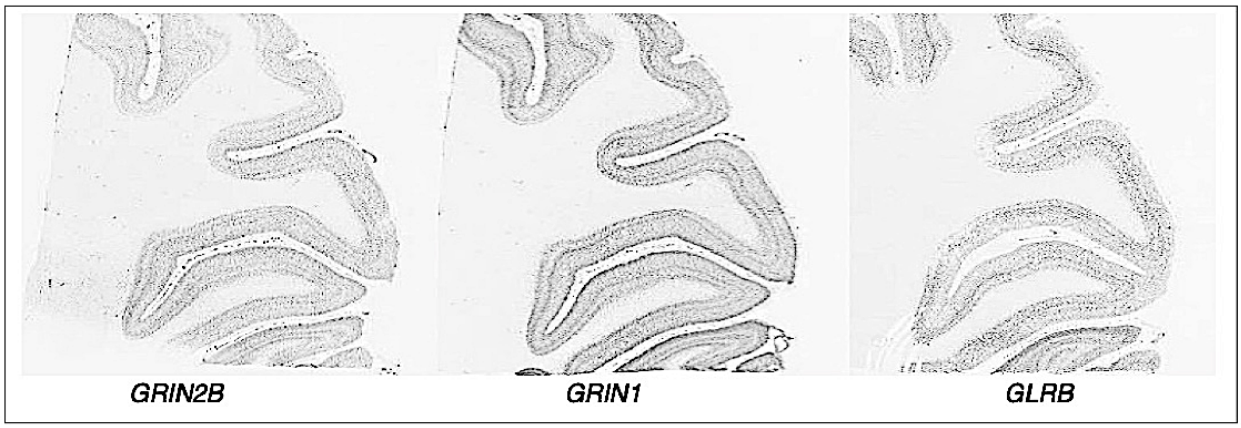

Frontal cortex

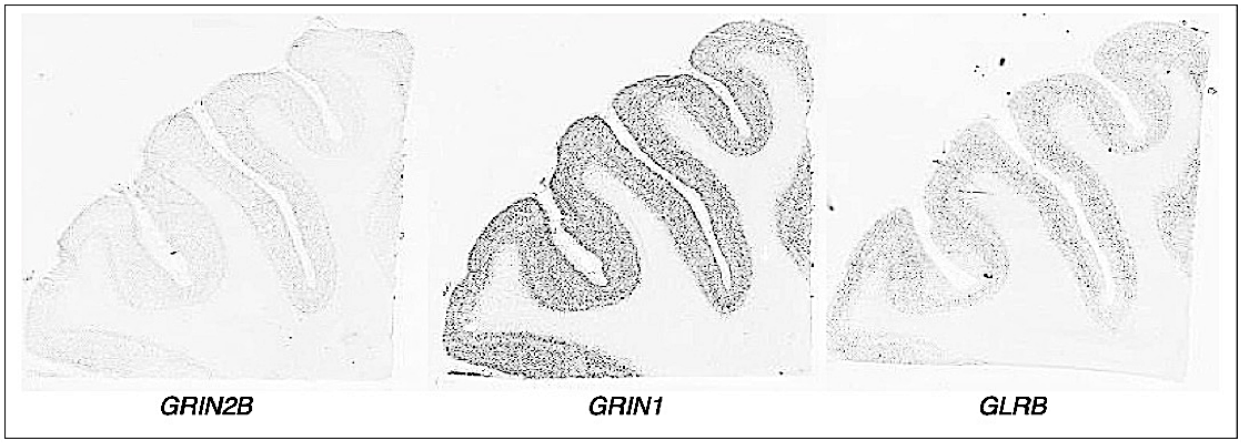

Dorsolateral prefrontal cortext

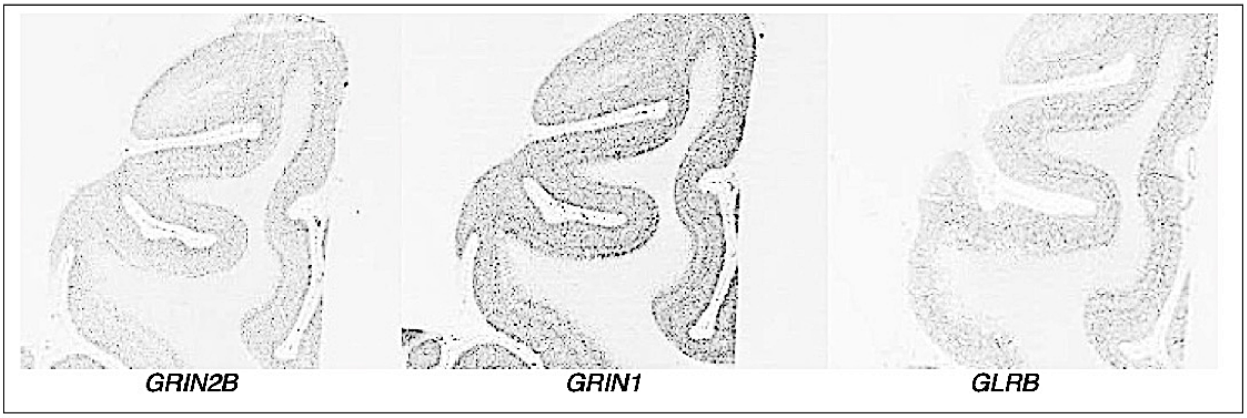

Additional Figure captions:

Supplementary Figure 4. GWAS SNPs from the ketamine glutamate receptor sub-network

Supplementary Figure 5. GWAS SNPs from the ketamine neuroplasticity sub-network